International Journal of Material Forming (2022) 15:41
https://doi.org/10.1007/s12289-022-01664-w

ESAFORM 25 YEARS ON

Advancements in extrusion and drawing: a review of the contributes by the ESAFORM community

Lorenzo Donati[1] · Barbara Reggiani[2] · Riccardo Pelaccia[2] · Marco Negozio[1] · Sara Di Donato[1]

Received: 10 December 2021 / Accepted: 4 February 2022 / Published online: 22 April 2022
© The Author(s) 2022, corrected publication 2022

Abstract
The present review paper would celebrate the 25 years anniversary of the ESAFORM association by summarizing the studies performed by the delegates of the ESAFORM conference series within mini-symposium "Extrusion and Drawing" and of the papers published in the International Journal of Material Forming in the same fields. The 160 analyzed papers have been divided in four main categories corresponding to the paper main chapters (Hot Metal Extrusion, Cold Metal Extrusion, Polymer Extrusion and Drawing) then further divided in sub-chapters in order to group them in more specific research subjects. The aim of this review paper is then to provide to the reader a complete overview of the investigated topics and of the research trends over the years within the ESAFORM associate researchers.

Keywords Extrusion · Hot metal extrusion · Cold metal extrusion · Polymer extrusion · Wire drawing · Drawing

Introduction

The global competition significantly altered the role of bulk metal forming processes within the panorama of manufacturing technologies in response to growing requirements for higher products complexities and higher production rates at continuously decreasing costs. The concomitant steadily increases in innovation and automation pushed metal forming processes to levels perfectly fitting with large-scale productions, still preserving their ability to generate sound, defect-free components. In this context, both extrusion and wire drawing have been often considered as versatile yet well-established mass forming processes. However, many significant advances have been made over the past 25 years which have been readily captured by a dedicated session of the ESAFORM conference and which have seen a continuous increase in the number or in the scientific level of the published papers. With the ambition to capture the major part of these advancements, the present review paper has been planned for providing to the reader a complete overview of investigated topics and research trends over the years within the ESAFORM community in the year of the celebration of the '25 years ESAFORM association anniversary'. Several trends can be captured in the evolution of ESAFORM researches within different subjects over the years. Firstly, a general increase in the complexity of experimental tests is evident, strongly linked to the progress in the capabilities of the equipment and of the measurement devices. Secondly, a more complete approach in the overall process analysis can be detected: in the early years, the papers were more focused on the analysis or estimation of a single output (such as the process load) and then evolved into the evaluation or optimization of multiple outputs at the same time. Third, experimental activities shifted from small-scale laboratory tests representative of the industrial process to a full-scale approach carried out in the laboratory environment or directly in the production lines. Last, but not least, a further common trend can be evidenced: if in the early

✉ Lorenzo Donati
1.donati@unibo.it

Barbara Reggiani
barbara.reggiani@unimore.it

Riccardo Pelaccia
riccardo.pelaccia@unimore.it

Marco Negozio
marco.negozio2@unibo.it

Sara Di Donato
sara.didonato2@unibo.it

[1] DIN Department of Industrial Engineering, University of Bologna, Viale Risorgimento 2, 40136 Bologna, Italy

[2] DISMI Department of Sciences and Methods for Engineering, University of Modena and Reggio Emilia, Via Amendola 2, 42122 Reggio Emilia, Italy

conference editions the papers were more focused on purely experimental testing campaigns or on the development of simplified numerical methods (analytical approach, upper bound approach or FE method) for process investigation, in the most recent editions the use of fully integrated thermal-plastic-structural FEM simulations have become a widely accepted method for process analysis and optimization.

The present paper is organized in four main sections: hot metal extrusion, cold metal extrusion, polymer extrusion and drawing. Each section has been then subdivided in further sub-sections to describe in more details the specific developments.

Hot metal extrusion

Hot Metal Extrusion refers to the efficient process used for the manufacturing of metal profiles taking advantage of the increased material ductility gained by the high temperatures involved. Even if generally considered a well-consolidated forming process, Hot Metal Extrusion is still strongly evolving in terms of developed technologies, extrudable alloys and end-user markets thus making it attractive for advanced researches aimed at increasing the overall process efficiency and at discovering further applications. Following these two research lines, topics that appealed the researchers attending the ESAFORM conferences have been divided in 11 paragraphs: the first 8 -paragraph 1.1 to 1.8- deal with the 'process optimization' (Die and Tools, Thermal Control and Semisolid Extrusion, Friction, Seam Welds and Defects, Microstructure Prediction and Control, Simulation Approaches, Constitutive Equations and Flow Stress, Metal Flow Numerical and Experimental Analysis) and the last 3 -paragraphs from 1.9 to 1.11- with the 'process development' (Composite Extrusion, Chip Extrusion and Profiles Bending).

Dies and tools

The die is the main tool involved in the extrusion process that is used to shape the final profile by the flowing of the material throughout its opening. Die design represents a key step in the process optimization since it strongly affects not only the die lifetime itself but also the profile quality and the overall process productivity. During its service life, die is subjected to critical thermal and mechanical loads that can lead to different types of failures mechanisms. In 2006, Mousoulis et al. [1] studied the premature failure of the mandrel part of an H13 die, designed to produce 40.000 kg of an aluminum profile but that fractured after only 500 kg. The authors realized only visual and microscopic inspections of the die and they gained the conclusion that fracture was caused by shearing stress in weak section thus evidencing an incorrect dimensioning of the mandrel ribs. In 2010 Irgens et al. [2] analyzed the effect of the insertion of a shadowing tongue with the aim to reduce the load acting on the main tongue used in case of U-shaped or semi-hollow profiles geometries. Authors evidenced by means of numerical simulations with DEFORM 2D code a decrease of more than 30% of local stress, even if accompanied by an increase of the overall extrusion force. In the same year, Reggiani et al. [3] compared two different numerical codes in terms of predictability of the stress level induced in a die during operation and proved the need of advanced constitutive models of the tool steel for a reliable estimation of die life and damage, as that proposed by the same authors in 2011 [4]. In 2021, Lechner et al. [5] performed an experimental–numerical (DEFORM 2D code) campaign aimed at investigating the level of residual plastic deformation (die deflection) in the proximity of the die bearings during high temperature CW024A copper extrusion. In this work, four tool materials (hot work tool steel 1.2367 and CS1, Ni-based 718, Co-Cr Stellite 1 alloy) were compared concluding that Ni-based alloy was the most suitable for the specific application. In addition to withstanding of the severe process loads, the die must be designed with the aim of generating sound profiles (defect-free, with high mechanical properties, within the required tolerances) and to guarantee the required level of productivity. Thus, many contributions reported in literature have been focused on the investigation of the effect of die geometric variables on these two process issues. In 2009, Donati et al. [6] experimentally tested the effect of four different pocket shapes, two different profile thicknesses and two extrusion speeds on the material flow inside the die showing a significant impact on the profile exiting velocities, especially at high speed (Fig. 1). Afterwards, in 2012, the same authors investigated and compared different strategies in balancing material flow during direct extrusion of an AA6082 hollow profile [7]. In more details, two different strategies were evaluated, one by the use of bearings, the other by the use of porthole area and position to correct and balance the flow. It was proved that the latter solution provided not only longest profiles but also less critical conditions in terms of surface quality, but with the counterbalanced effect of generating seam welds very far from bridge position thus being potential critical for final profile applications. In 2015, Negendank et al. successfully proposed an innovative axially moveable stepped mandrel to manufacture tailored aluminum (AA6060) [8] and magnesium (AZ31) [9] profiles with variable wall thickness in order to control the profile cross section dimension according to the expected loads applied during technical application. Accounting for the influence of the die elastic deformation on the product quality as consequence of the pressure applied by the material under deformation, in 2017 Biba et al. [10] developed in QForm VX a novel integrated numerical approach that

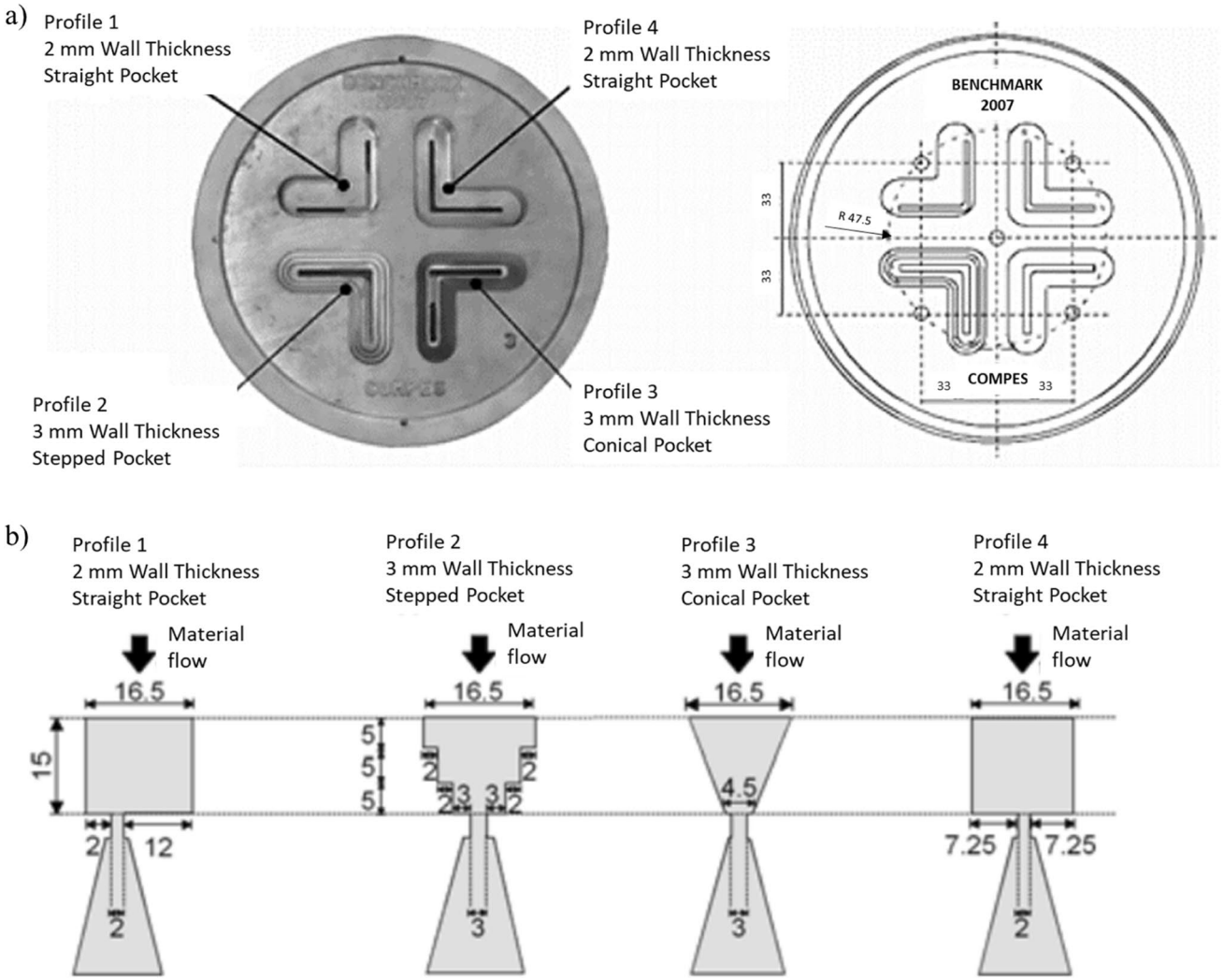

Fig. 1 a) Die and b) profile geometries investigated in [6] to assess the effect on the material flow.

couples the FE model of the material flow with the deformation and temperature distribution in the die. Recently, with the aim of finding solutions capable of simultaneously optimizing the die life, the quality of the product (avoiding thermally induced defects) and productivity, several works have been focused on the numerical and experimental investigation of die cooling. In 2014, Holker et al. [11] manufactured a novel die design concept with inner cooling channel by Selective Laser Melting (SLM) as well as by Layer Laminated Manufacturing additive technologies. The study used water as cooling media and revealed the potential of the solution in increasing the productivity of 300% for an AA7075 alloy. The cooling improved also the surface quality of the profile furthermore reducing the formation of coarse grains on profile surface. Following these results, in 2020 Pelaccia et al. [12] manufactured an H13 insert with a cooling channel by SLM, successfully testing its performances during the extrusion of aluminum AA6063 and magnesium ZM21 alloys cooled with liquid nitrogen. In addition, an innovative numerical model was developed in COMSOL Multyphisics coupling the extrusion process simulation with nitrogen cooling, showing error less than 7.5% if compared to experimental data. The model was then validated by the same authors on an industrial complex AA6060 profile cooled by liquid nitrogen flowing into a channel milled on the mating mandrel-die face [13]. The experimental–numerical matching returned again a very good agreement and encouraged the use of the model for a rapid channel redesign in order to attain a more thermal-balanced and productive die configuration.

Thermal control and semisolid extrusion

Proper temperature control is fundamental during the entire extrusion process, as the material properties, the final microstructure and the profile shape are strictly connected to the

management of the thermal problem. Several studies have been carried out in the past years for the investigation of the temperature distribution on the material during the process. In 2005, Moe et al. [14] carried out an experiment for the evaluation of the temperature distribution on AA6060 billets heated through electromagnetic induction before the extrusion process. The induction heating of billets was simulated by the finite element code Ansys to compare the results with experimental ones. Cooling subsequent to extrusion is also a crucial aspect of the process. In this context, Jäger et al. [15], in 2009, investigated the quenching process effected directly behind the die after curved profile extrusion (CPE). A forced air quench system was tested on extrusion of thin wall tubes in EN AW-6082 aluminum alloy. In 2010, Bikass et al. [16] studied through numerical simulation only the shape distortion due to non-uniform and asymmetric cooling by using Abaqus/Standard software in the extrusion of an AA 6082 aluminum alloy rectangular profile. In the same year, Farjad Bastani et al. [17] analyzed the isothermal extrusion process of aluminum by the use of the 3D finite element software Altair HyperXtrude and the 2D finite element software ALMA2π. They provided the best combination of process parameters and the so called "isothermal maps" for each phase of the press cycle (Fig. 2).

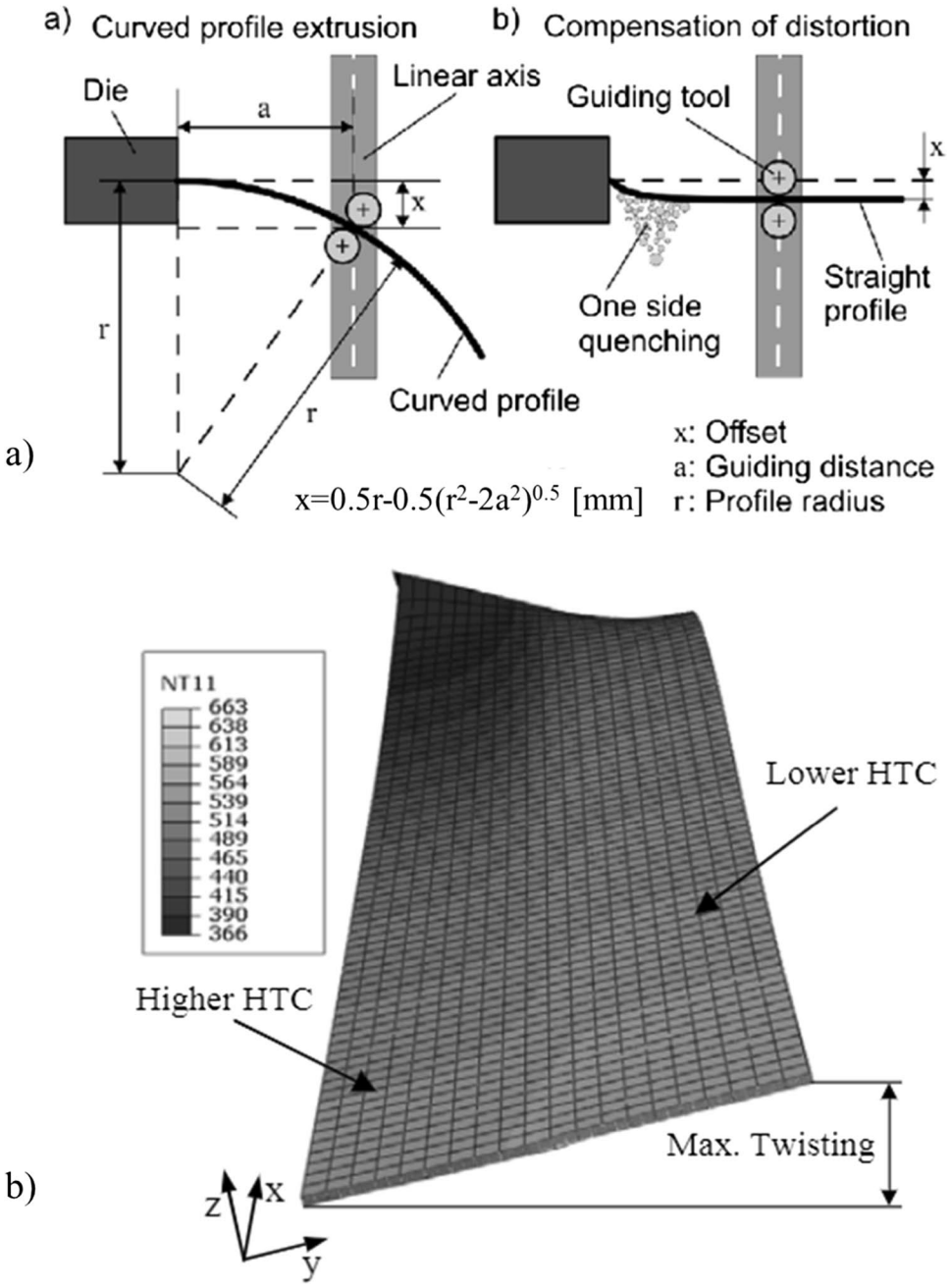

Fig. 2 a) Strategy for distortion compensate due to inhomogeneous quenching [15]. b) Temperature gradient (K) caused by asymmetric cooling condition [16]

The extrusion of heavy metal (i.e. copper or steel) involves high forming temperatures and high flow stresses. Semi-solid extrusion could be an alternative forming process due to the reduced flow stress. It combines the advantages of conventional casting and forging: forming has to take place in the semi-solid state, followed by a slidification step. In 2007, Neag et al. [18] carried out backward extrusion tests to examine the rheological behavior of a semi-solid Al-Si hypoeutectic alloy. With a mixed experimental–numerical method, by using the finite element code FORGE, they showed that Norton-Hoff model is insufficient to describe some characteristics of the semi-solid behavior. Two years later, Knauf et al. [19] studied the semi-solid extrusion applied to a ledeburitic cold working steel billet of X210CrW12. The experiments were performed by changing the main process parameters to detect their influence on the extruded products concerning chemical composition, microstructure and mechanical properties (Fig. 3).

Friction

Among the main difficulties for the development of a reliable numerical model of the hot extrusion process, the definition of the friction conditions at the material-tool interface plays a significant role. In 2005, Logé et al. [20] developed a small-scale extrusion method for the experimental determination of friction forces between the container and the billet. This method was applied to the extrusion of Zircaloy-4 (Zy-4) bars and tubes, while the rheological behavior of the material has been identified from uniaxial compression tests. Comparing the experimental activity with the numerical simulation by means FORGE finite element code, they identified a modified Coulomb law for an improved description of the friction at the billet-mandrel interface.

Few years later, in 2014, Sanabria et al. [21] investigated the friction boundary conditions during the extrusion process by using a new axial friction test, developed at the Research and Development Centre of UT Berlin. They studied the tribological behavior of aluminum alloy AA6060 and Magnesium alloy AZ31 against hot working steel 1.2344. The friction boundary conditions such as temperature, normalized normal stress and relative sliding speed were investigated and, in addition, the tested specimens were analyzed with OLM (Omnipresent Localization Microscopy) to investigate the variation in thickness of the shear zone and microstructure. The same experimental axial friction test was carried out in 2020 by the same authors [22], in order to investigate the thermo-mechanical behavior of the magnesium alloy AZ31B, to improve the constitutive modelling up to high strains ($\varepsilon > 1$). Moreover, friction tests were numerically simulated applying the FEM-based software DEFORM 2D. The Zener-Hollomon (Z-H) as well as the Hansel-Spittel (H–S) constitutive models, based on experimental data from hot compression tests, were evaluated during the simulations. From the comparison between experimental tests and simulation, a new strain-dependent multifunction model (SDM) was proposed.

Seam welds and defects

As any manufacturing process, also extrusion is characterized by a proper set of defects that are intrinsically related to the process set up (seam welds, charge welds and coring) or caused by an improper selection of process parameters (streaks, chevron cracks, tears and others). Among the former set, seam (longitudinal) welds are generated during the extrusion of hollow sections due to the material split around the legs of the mandrel and the subsequent re-joint to produce a continuous profile. This material behavior implies that any hollow profile, for each leg, is affected by welds that extend all long the entire profile length, thus explaining the wide literature on the topic. In details, published works on the topic have been focused on three main research lines: investigation on the effect of process and die-design parameters on welds quality, set up of novel testing experimental methods and development of advanced numerical models.

In 2005, Donati and Tomesani [23] tested samples extracted by H-shape AA 6082 profiles extruded with different die geometries and process parameters. The authors proved the influence of the welding chamber height and

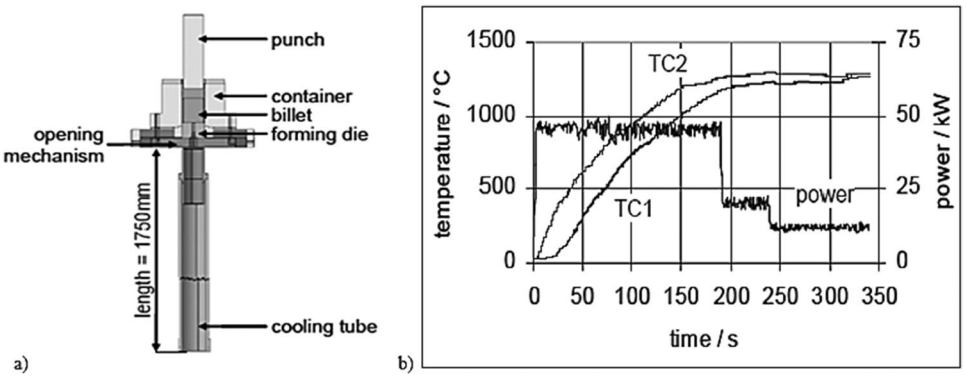

Fig. 3 a) Extrusion tool with installed cooling tube. b) Heating strategy and billet temperatures [19]

pressure for the achievement of sound welds. Moreover, it was also verified that elongation at fracture in tensile tests is the parameter most sensitive to welding conditions inside the die. The latter criterion was then used by the same authors, in 2007, to assess the better performances of blade shaped if compared to square shaped legs in the extrusion of an AA 6060 round tube [24]. Conversely, blade legs were most sensitive to creep failure mechanism in relation to the higher mean stress, as numerical assessed by the DEFORM 3D code. The level of achieved pressure and radial elongation at fracture in a bulge test was used in 2012 by Segatori et al. [25] to test a new die for magnesium ZM21 alloy designed to increase, by a more uniform strain, the production rate. In 2005, Ghiotti et al. [26] proposed a novel experimental procedure able to reproduce, at laboratory scale on a Gleeble machine, the welding of two streams in the typical industrial operating conditions of the extrusion process in terms of temperatures and normal-pressure-on-equivalent strain ratio. A different testing method has been set up by Valberg et al. in 2011 [27] to assess the seam weld quality based on a mandrel expansion test. In 2020, Dariusz and Pawel [28] developed an original device that shear and compress two alloy samples in a working movement under comparable conditions that occurs in the welding chambers. With fast computers and powerful programs developed in the first decade of 2000, the trend was mainly focused on investigating the extrusion seam welding by FEA, in order to predict actual state variables. Bonding mechanics in an AA6082-T6 aluminum profile were numerically and experimentally analyzed by Buffa et al. in 2007 and results discussed in terms of analogies with friction stir welding (FSW) solid state bonding [29]. In 2009 Ceretti et al. [30] presented a novel numerical approach able to simulate the real welding of the streams to avoid the persistent contact of the mesh elements, thus promoting a deeper understanding of the mechanism (Fig. 4). The model was used to investigate different die geometric configuration, corroborating the conclusion drawn by Donati and Tomesani in 2005 [23] on the impact of the welding chamber height on the seam welds formation.

Khan, Valberg and co-authors have done a significant contribution in the knowledge advancement of welds mechanisms in the extrusion process from 2009 to 2012. Important and in-depth information on how streams flow inside the mandrel ports [31] and on how this flow is affected by parameters like the shape of the legs (blade/pointed vs square) [32, 33] and port size [34] was gained by detailed analysis of numerical simulations (DEFORM code) and/or by comparing numerical outcomes with experimental data of visioplascticity (grid pattern analysis) (Fig. 5).

In 2012, Schwane et al. proposed a novel numerical method for the evaluation of the position and quality of seam welds in AA6082 profiles [35] and to account for a gas pocket in the welding chamber [36] by means of steady-state FEM simulations performed with the Altair HyperXtrude code. Accounting for the process complexity and the difficulties to manage all the involved variables, Gagliardi et al. [37], in 2017, suggested to adopt the Taguchi/ANOVA techniques in order to reduce the required number of simulations for the evaluation of the influence of twelve geometric variables on two selected responses (load and pressure in the welding chamber). As previously highlighted, other than seam welds, also charge welds (front-end) and coring (back-end) defects are intrinsically related to the extrusion process mechanism. Differently from seams, charge welds, generated due to the billet-to-billet interaction, affect only the new-old billet transition zone of the profile. However, a further difference is that charge welds are usually marked by much lower mechanical properties than the base material due to the interface contamination, thus requiring to be discarded for critical applications. Coring defect, instead, caused by the inflow of contaminated skin of the billet toward the core during the extrusion cycle, can be avoided if a proper discard length is selected for each billet. In 2020, Valberg et al. [38] applied FEM (DEFORM 3D code) and experimental grid pattern analyses to deeply investigate how contaminated skin inflow occurs and how subsurface layers flow behave with respect to the history of deformation. In the same year, Negozio et al. [39] simulated, with Altair HyperXtrude code, two industrial profiles made of AA6063 and AA 6082 aluminum alloys to predict front end and back-end defects and compared the achieved results also with the theoretical models available in literature to evaluate pros and cons of each approach.

Microstructure prediction and control

In the last decades, lightweight alloys increasingly gained industrial interest in the almost all industrial sectors

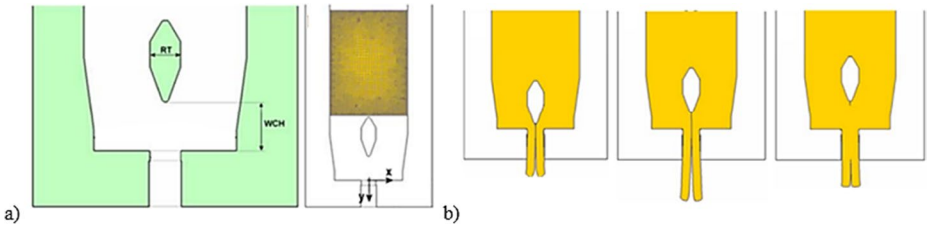

Fig. 4 a) Geometrical parameters investigated in welding formation (WCH: welding chamber height, RT = rib (leg) thickness) and the simplified 2D FEM model developed in DEFORM 2D; b) weld behavior with different WCH values [30]

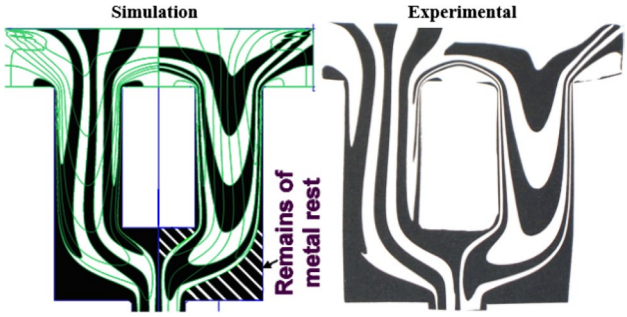

Fig. 5 Numerical-experimental comparing of metal flow when extruding through filled die using a square leg [31]

including automotive and aerospace. The mechanical properties are deeply affected by the microstructure, and consequently, research activities became of increasing interest in order to investigate the influence of process parameters on the grain size evolution and to develop microstructure prediction models. These activities challenged the lightweight alloys research community, in particular for the study of the microstructural behavior of aluminum and magnesium alloys. Concerning magnesium alloys, in 2010 and 2011, Gall et al. [40, 41] studied the effect of different extrusion temperatures on the microstructure of AZ31 plate profiles, in order to investigate the influence of the anisotropy on the mechanical proprieties. The authors found that the anisotropy is linked to the developed texture, which allows the activation of specified deformations modes in defined directions. In 2011, Ge et al. [42] studied the grain size evolution of AZ31B and ZM21 alloys during hot compression and laboratory-scale extrusions for the understanding of the influence of billet pre-heating temperature and strain rates on the recrystallized grain size. In 2018, Jaehnke et al. [43] combined and integrated the extrusion and the equal channel angular pressing (ECAP) in a single extrusion die, in order to decrease the anisotropy and the strength differential effect (SDE) through modification of the texture compared to conventional extrusion process. In 2019, Tomovic-Petrovic [44] studied the effect of Ni on the mechanical properties and formability of AZ91 alloy, combining experimental investigations and FEM analysis during extrusion trials. Concerning aluminum alloys, studies were performed comparing experimental investigations with the results of FEM simulations. In 2006 and in 2009, Fitta et al. [45] integrated into commercial FEM codes a physical model based on dislocation density, subgrain size and misorientation angle and they studied the influence of the substructure on the static recrystallization of a AA2024 alloy. In 2008, Krumphals et al. [46] carried out extrusions of AA6082 profiles and the data obtained were used to validate an integral finite element model and to assess the relative importance of the extrusion parameters on the microstructure of the profile. The use of the FEM for the investigation of the microstructure evolution was also made by Parvizian et al. in 2010 [47], with the aim of demonstrating the sensitivity of the grain size of an extruded AA6060 profile to processing conditions (Fig. 6).

In 2011, Segatori et al. [48] compared the experimental results of extrusions made at different process conditions of an AA6082 profile to the results of FEM analysis, thus proving that there is no influence of process temperature and ram speed on the dynamic grain evolution. In 2007, Sanabria et al. [49] carried out sticking friction experiments to understand the impact of temperature and sliding speeds on the sub-surface deformation and microstructure of a AA6060 alloy. The authors found that a severe deformation occurs below the friction surface, which is distinguished to the adjacent slightly deformed dendritic grains and quantified the thickness evolution of the high shear deformation zone.

Simulation approaches

In the aluminum extrusion sector, FEM codes have become one of the most important tools for process and product optimization. The complexity of the process, the high extrusion ratio and, consequently, the long simulation times with pure FEM lagrangian approach, led to an evolution over the years of the numerical tools and methodologies to gain accurate solving capabilities at reduced computational times. Different numerical approaches and methodologies have been proposed over the years in order to study the issues of the process or to exceed the limit of existing numerical model. In 2008, Koopman et al. [50] used an Eulerian approach

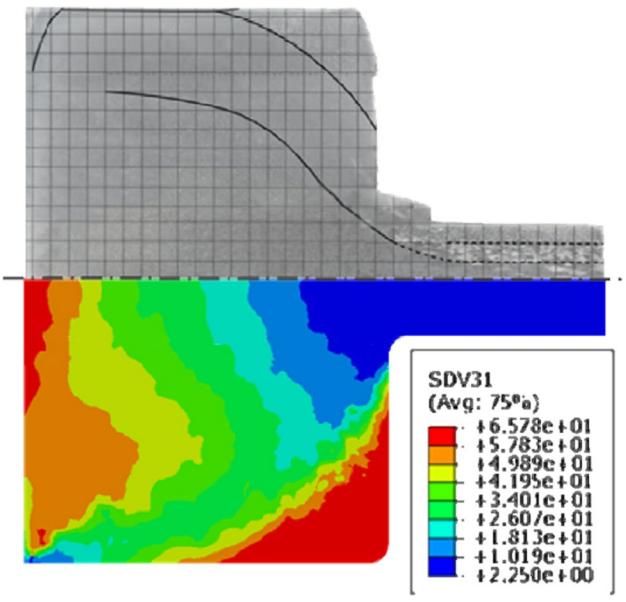

Fig. 6 Experimental and simulation results for evolution of grain size during extrusion of aluminium alloy 6060 (the simulation results are non-dimensional and normalized by saturated grain size) [47]

combined to the smooth original coordinate function with the aim to study the die filling and the flow front at the die exit (Fig. 7). The experimental–numerical comparison with the extrusion of AA6063 round profiles showed a quite good matching in terms of flow front although no die deflection was taken into account.

In 2009, Alfaro et al. [51] proposed the simulation of round tube profile with the Natural Element Method (NEM) to investigate the formation and the quality of the seam welds. The comparison with the real experimental test confirmed the good prediction of the welding behavior during the extrusion process. In 2007, Abrinia and Makaremi [52] studied the three-dimensional problem of the extrusion of elliptical profile using the upper bound theory. The analysis of shaped sections with larger dimensions than the initial billet was performed by varying the extrusion ratio, the die length, the friction condition and the shape complexity. W. Two years later, Assad et al. [53] studied the boundary conditions applied on bearing corner nodes to satisfy the flow conservation condition in the Eulerian formulation. Again in the years 2008 and 2009, Ertürk et al. [54, 55] proposed a modification of the phenomenological Cazacu and Barlat model to consider the strain rate and the temperature dependency on flow behavior of magnesium alloys. Indeed, due to the hexagonal closed packed crystallographic structure, the magnesium alloys show mechanical anisotropy and tension–compression asymmetry if compared with aluminum alloys. The coefficients of the model were calibrated for ZEK 100 magnesium alloy by means of hot compression test, then the flow stress law was implemented into the commercial software Abaqus/Explicit to simulate an indirect extrusion of a round bar. Several works were presented about the study of the extrusion process in terms of material flow, thermal field and die deflection with the aim to present the improvement of FEM codes as supporting tools for the process design in the industrial framework. In 2010, Donati et al. [56] compared six different FEM codes in the simulation of two overlapped AA6082 U-shape profiles: one with fully supported opening, the other with partially supported opening. The experimental–numerical comparison showed a good codes prediction in terms of thermal field and extrusion load, but some limits emerged in terms of die deflection prediction (Fig. 8). In 2011 and 2012, Biba et al. [57, 58] showed the increased accuracy of the software QForm Extrusion by taking into account the influence of the die deformation on the material flow through the die. The comparison with different experimental case studies showed that the die deformation causes the alteration of the bearing area and the friction condition, thus influencing the material flow. In 2017, Kronsteiner et al. [59] compared the Update Lagrangian method (DEFORM code) with the Arbitrary Lagrangian Eulerian method (LS-DYNA software) for the extrusion process of AA6082 tube profiles. One of the major advantages of the ALE method concerns the overcoming of the contact problem of the mesh elements in the welding chamber obtained through the preparation of Eulerian mesh elements representative of the billet, the die and the extruded profile already at the beginning of the simulation.

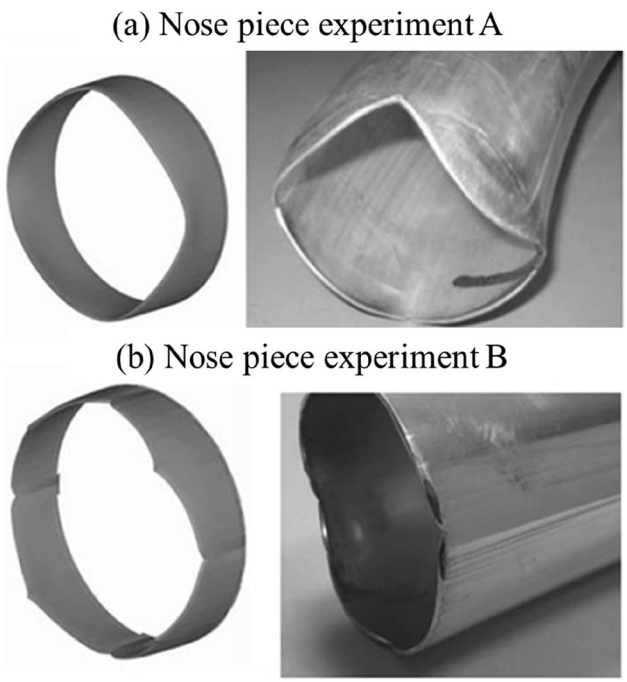

Fig. 7 Experimental–numerical comparison of nose pieces. The experiments were carried out using two different dies: a) die with little undercut in the mandrel and a bearing length of 5 mm; b) die with big undercut in the mandrel and a bearing length of 3 mm. [50]

Finally, some works were focused on the virtual optimization of the extrusion process, testing a large number of variables in an automatic way. In 2010, Caseiro et al. [60] used three different optimization methods to design an integrally stiffened panel (ISP) subjected to buckling for aircraft applications. The simulation of the buckling was performed by means of Abaqus software. The algorithm based on a Hybrid Differential Evolution and Particle Swarm Optimization attained the lower values for the cross-sectional area, leading to the better ratio between the buckling load limit and the structure weight. In 2013, Siegbert et al. [61] tried out an optimization framework on the extrusion of L-shaped profile using the balancing of the exit profile velocity as objective function. The geometry parametrization allowed to test different geometry features based on die maker experiences in automatic way.

Constitutive equations and flow stress

Together with friction, the definition of accurate flow stress data is a critical task for the development of reliable

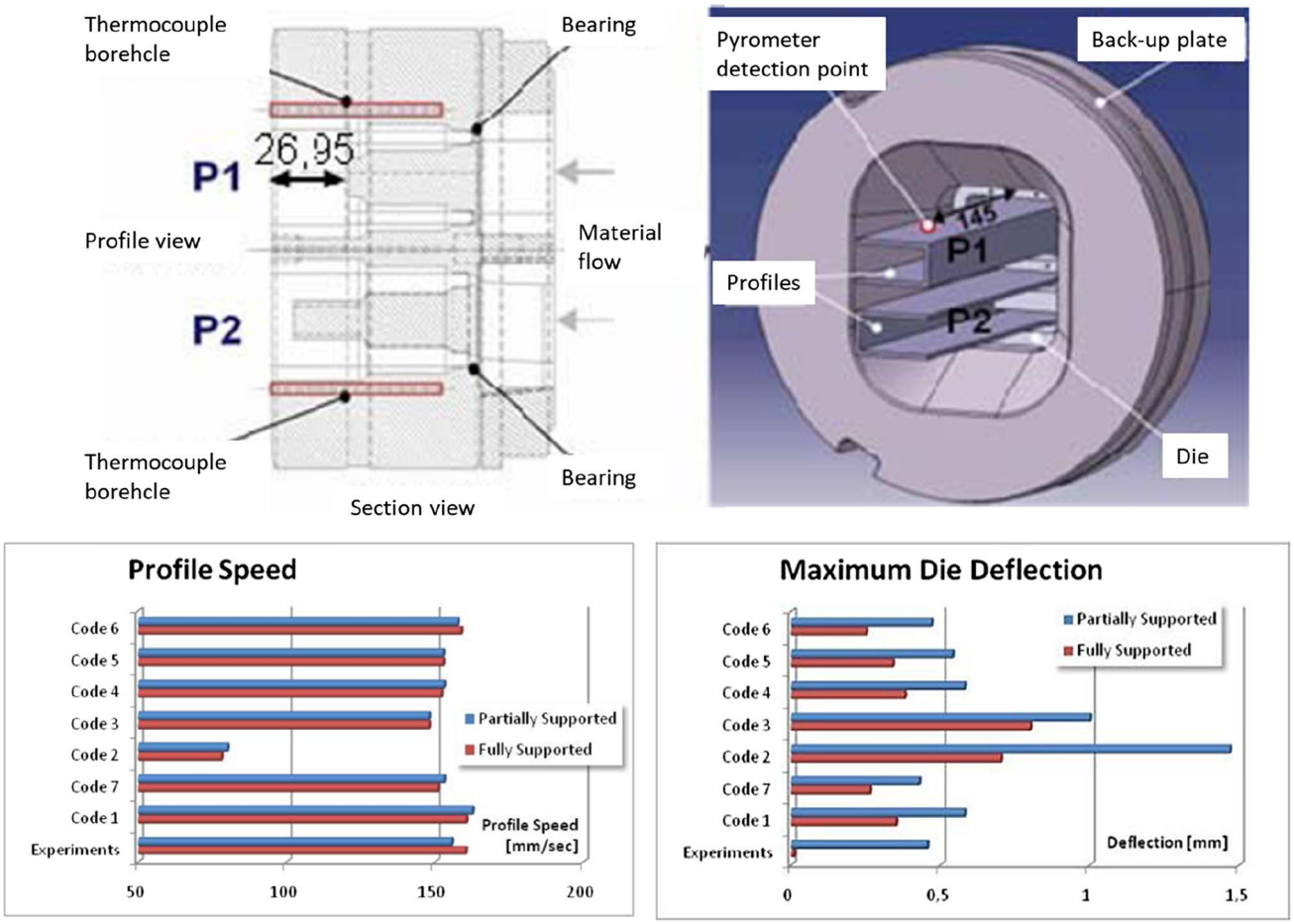

Fig. 8 Comparison between six different FEM codes and the experimental results in terms of profile speed and die deflection [56]

numerical simulations. Flow stress data can be characterized by means of different testing method (tensile test, compression test, torsion tests) in the temperature, strain and strain rate range of the process under analysis. The hot torsion test allows to obtain the material flow characterization at high temperature, strain and strain rate typical of the hot extrusion process, overcoming the limits of the other tests especially in terms of achievable maximum strain. In 2011, Donati and El Mehtedi [62] characterized the flow stress of AA6082 by means of hot torsion test: four different alloys belonging to the 6082 nominal standards were tested to analyze the differences in terms of flow stress behavior influenced by differences in chemical composition, evidencing that is not possible to identify a single flow stress behavior for the whole AA6082 class. In addition, the procedure to obtain the parameters for sinhyperbolic flow stress to be implemented within the FEM codes is presented and discussed. In 2012, Bruni and El Mehtedi [63] presented a new multivariable regression analysis starting from the hot torsion characterization of ZEK 200 magnesium alloy in the temperature range of 150–450 °C. The division of the temperature range into two classes (150 °C-300 °C and 300 °C-450 °C) made it possible to obtain a better accuracy over the experimental data respect to the regression with a single temperature range (150–450 °C) thanks to the reduction of the parameters in the equation.

Metal flow numerical and experimental analysis

The main challenge in hot metal extrusion is achieving an equal exit speed in all sections of the profile. Indeed, complex interactions between die design, friction conditions and material viscosity usually produce an unbalanced exit speed thus generating different types of defects (surface tears, thinning of the profile and aesthetic defects) that severely limit the productivity of the process. The interaction of these phenomena is too complex to be modeled with analytical approaches and only the development of reliable FEM simulations has allowed to investigate this specific aspect. In order to evaluate the accuracy of the simulation on this issue, several articles have focused their attention on the experimental investigations and simulations of the metal flow

during metal extrusion. In 2006, Valberg et al. [64] used a commercial FEM code (DEFORM code) to analyze the indirect hot extrusion of AA6082 alloy. Important information on the metal flow were achieved by comparing the numerical results with the grid patterns in the butt after experimental tests. The studies on the extrusion of the AA6082 continued in the following years, from 2010 to 2017, thus consolidating the knowledge on the reliability of FEM simulations with DEFORM software of the process (Fig. 9) [65–67].

In 2006, Hansson [68] investigated the numerical prediction of the process load thus comparing experimental measurements made on the extrusion of stainless-steel round bars with the results of the FEM simulations using the Lagrangian code MSC.Marc. In 2007, Koopman et al. [69] compared the metal flow obtained by experimental tests on the extrusion of aluminum billets with the results of FEM simulation (software DiekA) integrated with a method for determining the frontlines inside the container and the die based on the steady-state velocity field. In 2005, Manninen et al. [70] studied the flash formation during OFHC (Oxygen-Free High thermal Conductivity) copper with Conform extrusions under different process conditions, developing an analytical model validated with FE-analysis using the Abaqus/Explicit code. In 2005, Wajda et al. [71] examined changes in temperature and pressure during strip extrusion of AA6060, providing information useful for the development of thermo-mechanical models of material flow. In the same year, Baron et al. [72] developed a numerical model into a commercial FEM code, which consists of the pre- and postprocessor PEP and the solver LARSTRAN/SHAPE, validated by comparing the results of the simulation to the data acquired during experimental extrusion tests on a ZM21 alloy. In 2009, Pathak et al. [73] studied the material modelling combined to the die and process design of rod extrusion of γ iron, using the finite element analysis (MSC Software) to find and test the optimized design, evaluating the stress, strain distributions and load requirements. In 2010, Valberg [74] described the importance of tracking back profile points during direct and indirect extrusions by means of a new approach that he named as "emptying diagrams". In 2011, Y.A. Khan et al. [75] carried out extrusions with different portholes sizes and used the grid pattern technique to characterize the metal flow of AA6005 alloy. The results were compared to the outputs of 3D simulations using DEFORM software thus further proving the importance and the reliability of the grid pattern technique to characterize the boundary conditions of real experiments. In 2012, J. Kandis et al. [76] experimentally investigated the two-hole extrusion of two alloy, AA6063 and AA7108, and compared the results with FEM metal flow analysis using the DEFORM code. In 2013 and 2014, Khorasani et al. [77, 78] highlighted the differences between the theoretical velocity field obtained by Avitzur model and the one simulated by DEFORM code on direct, indirect and friction assisted extrusion. The velocity field was also studied by Valberg et al. [79], in 2014: the authors conducted an accurate FEM analysis with DEFORM code to understand the metal flow in case of asymmetric portholes. In 2016, Kronsteiner et al. [80] presented an innovative non-destructive method for the analysis the metal flow of an AA6082 through the use of a billet copper coating and subsequent computed tomography analyses. In 2018, Chen et al. [81] simulated a AA6063 alloy extrusion using the Altair HyperXtrude software of an asymmetric die and validated the results with experiments thus proving the reliability of the code. Moreover, the scheme of the die correction and optimization were discussed. In 2018, Galliac et al. [82] studied the production route of Zirconium alloy cladding tubes for nuclear applications. Manufacturing route was optimized by modelling of hot extrusion and cold pilgering processes with FORGE software. The cladding tubes non-acceptance ratio coming from surface defects was reduced by the mastering of the microstructure and surface quality of the extruded tubes, together with the optimization of the pilgering tools geometry. In 2018 and 2019, Valberg et al. [83, 84] investigated the metal flow and temperature conditions during industrial size extrusions of AA7108 alloy at different process parameters using FEM analysis

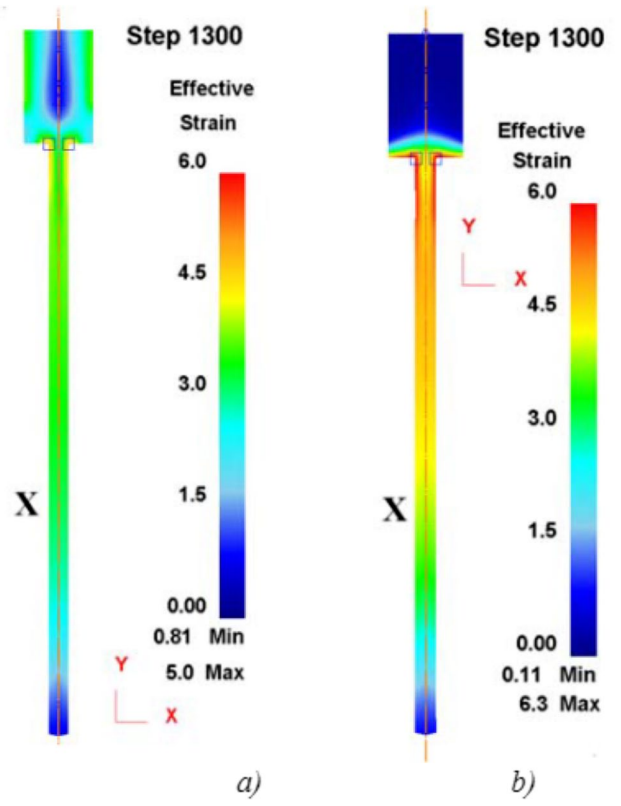

Fig. 9 Effective strain distribution from simulation; a) direct and b) indirect extrusion [65]

(DEFORM code). In 2021, Habans et al. [85] developed a numerical model of the hot extrusion process using the FEM code FORGE NxT with experimental data from literature and used it to assess the feasibility of the extrusion of a large seamless hexagonal 9% Cr—1% Mo steel tube.

Composite extrusion

The topic deals with the development of hybrid structural components with the aim to exploit the combination of advantageous mechanical, physical or chemical properties of various materials within a single component. The papers presented during the ESAFORM conferences can be divided based on the different objectives to be achieved with the co-extrusion process: the co-extrusion of bilayer billet to obtain different properties in the core and in the surface, the co-extrusion of a mixture powder, the lateral angular co-extrusion to realize hybrid steel-aluminum tube and the co-extrusion of billet reinforced with continuous/discontinuous steel element to increase the mechanical strength of lightweight components (Fig. 10).

In 2021, Chen et al. [86] studied a process chain of compound casting and co-extrusion of AA7075/6060 bilayer billets to obtain hybrid components with strength in the core (AA7075) and good corrosion resistance in the shell (AA6060). Compared to the as-cast components, the hot extrusion ones showed high homogenization of the interfacial bonding, reduced voids and higher shear bonding strength (from 93.8 MPa to 145.9 MPa). In 2013, Negendank et al. [87] studied the indirect co-extrusion of assembled billets with the core in AZ31 magnesium alloy and the shell in AA6060 or AA6082 aluminum alloys. The macroscopic observation of the coextruded rods provided a good surface quality independent from the investigated extrusion ratios (R = 24:1 and R = 41:1). The crack generation at the interface seemed to be caused by the different material flow velocities between the core and the shell as suggested by the FEM analysis of the process realized with DEFORM code. Finally, the push out test showed shear strength higher for higher extrusion ratio (an average of 65 MPa against an average of 36 MPa). In 2006, Sliwa [88] analyzed the metal flow in the co-extrusion of PbSb3 (core) and pure Pb (sleeve) using flat, conical and convex dies. The results showed that the use of convex die led to more homogenous flow of the layers of the composite material. In a different context, Negendank et al. [89], in 2021, tested the extrusion of a mixture of pure aluminum powder and graphene nano platelets (GPN) in contents of 0.5%, 1.0% and 1.5%. The powder mixtures, produced with EIRICH mixer, resulted in homogenous GNP dispersion. The surface quality of the extruded rods decreased with increasing GNP content but increased for higher extrusion ratios. In addition, the use of conic die resulted in better surface quality compared with the flat face die. In their works from 2017 to 2020, Thürer, Behrens et al. [90–92] realized hybrid tubes on an industrial scale with the core in AISI 5120 steel or in 20MnCr5 and the

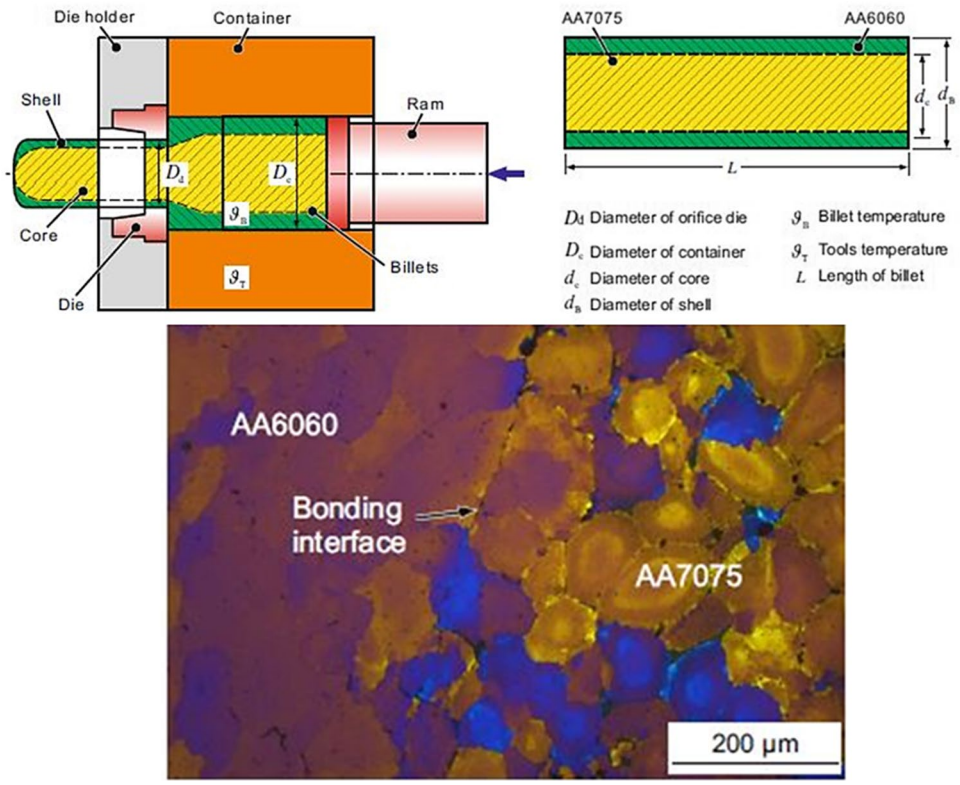

Fig. 10 The co-extrusion of bilayer billets [86]

shell in AA6082 aluminum alloy by using the lateral angular co-extrusion (LACE). The steel tube was inserted into the extrusion die at an angle of 90 °C to the extrusion direction, where it was covered by the aluminum. The obtained profile was very straight with no significant diameter changes, no waviness and no microscopic gaps in the aluminum-steel interface. The break-up of the initial oxide layer present on the aluminum was required to obtain a close bond to the steel. The pre-heating of the steel seemed to be necessary to establish the bonding during the LACE process. The validation of the numerical model of the LACE process by means of commercial software FORGE NxT was also presented in [91, 92]. In the years 2011 and 2012, Foydl et al. [93, 94] performed a co-extrusion process, where E295GC steel reinforcement elements were inserted into convectional AA6060 and AA6082 aluminum billets. Different shapes, dimensions and positions of the steel reinforcement were tested. It was found that the position of the reinforcements was influenced by the initial position in the billet, their length and the extrusion ratio, but not by the extrusion speed and the temperature of the billet. In addition, the forging of the co-extruded components was proved for the continuously reinforced products with X10CrNi18-8 wires. About the high reinforcing volume with steel wires, Pietzka et al. [95], in 2013, tested the extrusion of AA6060 alloys billets reinforced with X10CrNi18-8 wires fed through the bridges of a special porthole die. The paper reported the results in testing different die design and different strengthening strategy. A profile with a reinforcing volume of 13.5% was successfully manufactured and a first process window for this co-extrusion process was assumed.

Chip extrusion

The great interest in the recycling of material scraps, especially due to the high energy required to obtain primary aluminum, has led to several works presented during the ESAFORM conferences on the hot chip extrusion. A great deal of material is lost within the production cycle of mechanical components realized by chip removal process. Chip is a kind of scrap difficult to recycle by conventional re-melting process with an average material loss of 20–50% due to the contamination with oxides and machining oil. In addition, the high-energy consumption of the melting process may suggest the investigation of the recycling of the chips directly by hot extrusion, which requires only the 10% of the energy required by the re-melting. In 2010, Güley et al. [96] used material scraps in AA1050 in the shape of small pins and chips in AA6060 resulting from a turning operation to extrude a full rectangular profile (20×5 mm2) at 500 °C (Fig. 11). Chips and pins were preliminary degreased then cold compacted in cylindrical billet shape: a mixture of chips and pins and only 6060 chips were tested. The tensile test evidenced the same true stress-true strain curve for 6060 chips and the as-cast billet, while an intermediate strength between the value of source materials was found with the AA6060-AA1050 mixture billets.

In 2017 and 2018, Paraskevas et al. [97, 98] performed the recycling of AA6060 machining chips within the industrial production line, extruding a single solid profile bar (101.0×10.1 mm2) at 480 °C, after the degreasing and the cold compaction of the scraps. In the first work [97], the authors used a 2-porthole die and the tensile tests showed 32% of improved ductility and 40% of lower strength compared to the cast-based reference profile due to the coarser microstructure obtained. Instead, in the second work [98], the use of 4-porthole die introduced additional plastic strain into the profile and thus, higher grain refinement, higher mechanical strength, less ductility, enhanced solid state bonding/welding and less surface defects. The limit of the study is related to the introduction of additional plastic strain in the profile by means of porthole dies that normally is extruded through a simple flat die. In 2016, Buffa et al. [99] investigated the recycling of AZ31 magnesium alloy chips through the Friction Stir Extrusion. The combination of the ram pressure and the die rotation produced both the heat and the pressure to compact and extrude the scraps as a consolidated rod. Six different conditions were tested, varying the tool rotation speed (300, 500 and 700 rpm) and the extrusion ratio (5 and 3,57) as reported in Fig. 12. The higher tool rotation speed generated sound extruded rod with a mechanical resistance of about 80% of the base material. In this context, El Mehtedi et al. [100], in 2018, used the Friction Stir Extrusion to recover AA1099 machining chips. The numerical analysis with the commercial software DEFORM 3D and the experimental trials confirmed that a high rotational

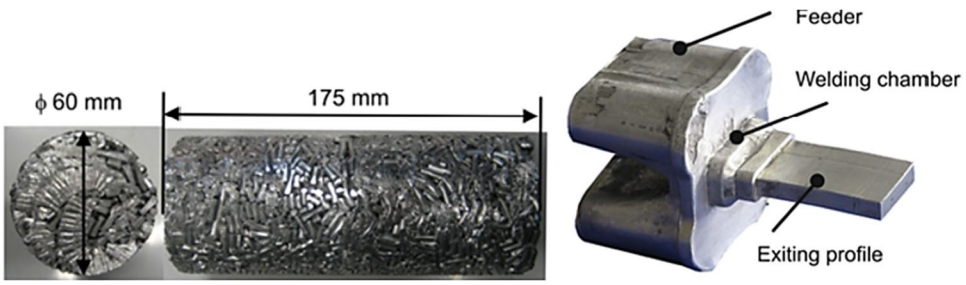

Fig. 11 The hot extrusion of billets realized with compacted AA1050 and AA6060 chips [96]

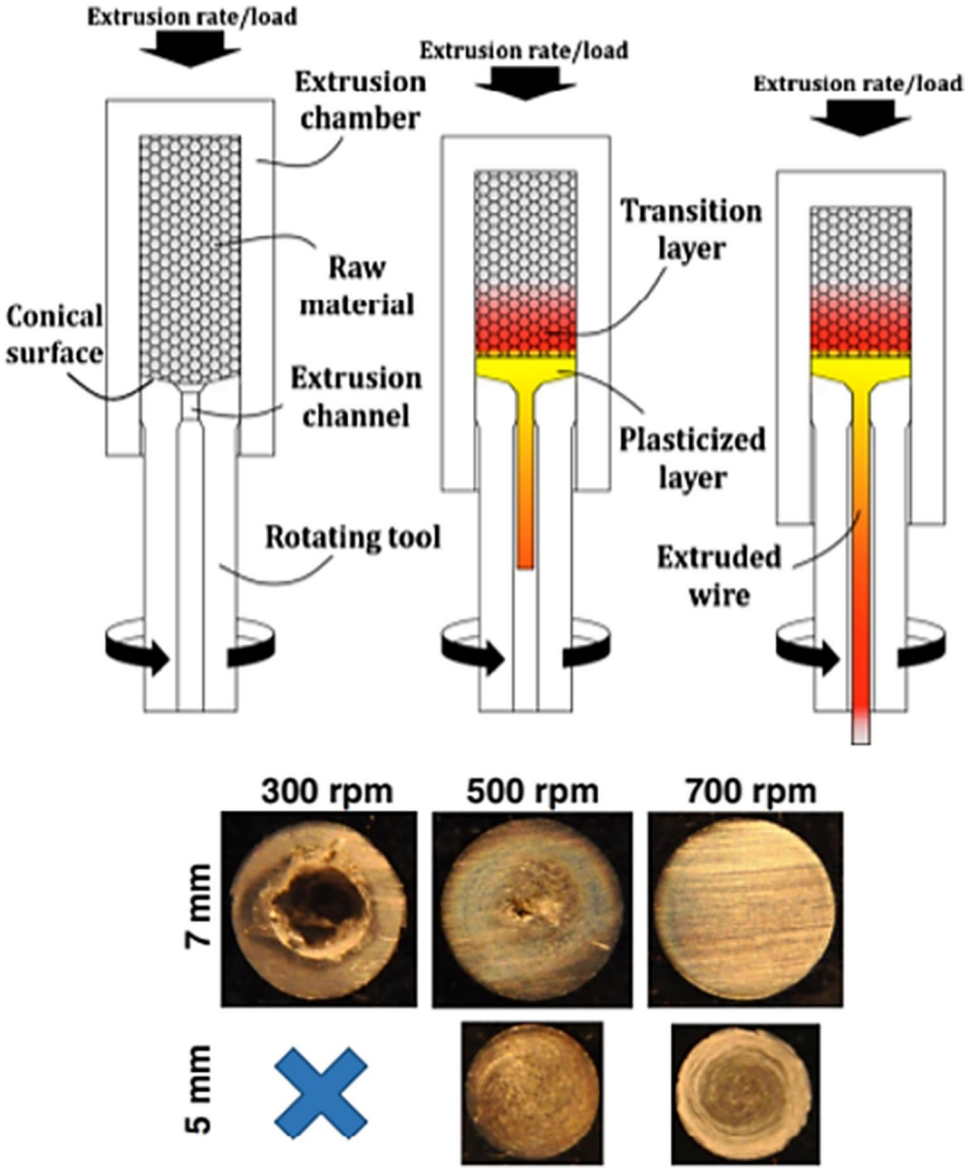

Fig. 12 Recycling through friction stir extrusion process varying the rotational speed and the diameter of the profile [99]

speed (1000 rpm in this case) was necessary to produce a sound round profile.

In 2012, Widerøe and Welo [101] analyzed the material flow of AA6060 granulate (3 mm of diameter and 8 mm of length) in a screw extruder using a contrast material. The rotation of the screw (10 rpm) guaranteed the compaction of the granulate, while the extrusion began when the pressure increased for the filling of the extrusion chamber. The results showed that the newly fed granulate first displaced material in the center of the screw channel, pushing pre-existing material further down the channel towards the extrusion chamber. The dead zones were mainly identified at the bottom of the screw channel and in the corners of the extrusion chamber. In the following year, Widerøe et al. [102] developed a new testing machine to characterize in a simplified manner the process parameters of the screw extruder in terms of rotational speed, extrusion load and temperatures for achieving sound profiles.

Profiles bending

The manufacturing of lightweight components for support structures in the automotive and construction fields represents an interesting challenge for engineering researchers and technicians. In this context, the production of curved profiles is required due to geometric and aerodynamic specific requirements. Especially in the automotive field, these requirements can be extremely strict and difficult to be achieved by using the conventional bending procedures. Consequently, the definition of new or improved manufacturing techniques combined with controlling methods were investigated by some researchers and presented at

ESAFORM. In 2007, Chatti and Kleiner [103] investigated innovative procedures, for the production of straight and curved profiles, developed at the Institute of Forming Technology and Lightweight Construction (IUL) of the University of Dortmund. Among these new procedures, methodologies for bending of profiles made by tailor rolled blanks, of tailored tubes and the curved profile extrusion were presented and analyzed in order to understand their applicability, feasibility and the improvements in terms of achievable product requirements. In the same year, Moe et al. [104] studied optical measurements techniques to be used for the in-line shape control in combination with the internal pressure during pure bending experiments on a AA6060 alloy material. The use these techniques, based on white light stripe projection, allowed to analyze the onset of sagging, buckling and spring-back phenomena.

Cold metal extrusion

Cold metal extrusion is a research topic in-between hot metal extrusion and cold stamping as the process makes components starting from room temperature workpieces, then deformed by a punch and a set of tools to make components with a deeply elongated shape in the "extrusion" direction. A way to discriminate among cold extrusion and forging is made by considering friction forces: if the friction forces are mainly oriented in the same direction of the tool movement, we refer to forward or backward extrusion otherwise we are generally dealing with a forging process. The contributes of the ESAFORM researchers within the Cold Metal Extrusion subject strongly evolved within the years: if in the early conference editions, the papers were more focused on purely experimental testing campaigns or on the development of simplified numerical methods for process analysis, in the most recent editions the use of fully integrated thermal-plastic-structural FEM simulations have become the most widely accepted method for process investigation and optimization. Indeed, almost all recent papers use FEM codes as tool for generalization of the results of a specific experimental campaign. Cold metal extrusion topics widely investigated by ESAFORM researchers are: tribology aspects of the process (including evaluation of tool coating effects or evaluation of lubricant efficiency), prediction of chevron crack defects through damage models, residual stress onset during cold forming or innovative process development (like ultrasonic extrusion, micro-extrusions or bimetallic cold-welded components). Research studies in the field of Cold Metal Extrusion have been then divided into 9 subjects that can be grouped into two main categories: Process Analysis -paragraphs from 2.1 to 2.4- and Process Developments -paragraphs from 2.5 to 2.8-.

FEM simulations

The need to replicate, or predict, the evolution of processing conditions in cold forming operations has produced a wide literature on the use of numerical methods for process analysis. Since the first edition of the conference, the most investigated numerical methods have been upper bound techniques and FEM analyses, being the latter the one with greatest application over the years. In 2005, Ma and Barnett [105] presented an approximate upper bound solution for forward extrusion through a rotating conical die. The authors developed a model that took into account the material twisting inside the container and the circumferential slippage at the tool/workpiece interface thus providing coherent trends on extrusion load reduction but the paper lacked to validate the results over specific experimental verifications. In 2005, Skakun et al. [106] applied the upper bound model and the FEM approach through MSC Marc Software in the radial extrusion of an Aluminum gear section under different gear flank configurations. The authors compared the extrusion load predicted by the two approaches with experimental results and they found a reasonable agreement between upper bound and FEM with experimental data but the UB method evidenced a great discrepancy in the final stage of corners filling. Two years later, Pepelnjak et al. [107] applied FEM code Abaqus in the analysis of the inner race component of a constant velocity joint to be produced by the sequence inverse extrusion and fine coining in a near-net-shape approach. The influence of tool redesign was analyzed to evaluate the robustness of the forming process in order to stabilize the production around the mean value of prescribed narrow shape tolerances on a 1/12 section of the component. The loading conditions of the dies was experimentally and numerically investigated by Plancak et al. in 2006 [108] during the backward extrusion of a C15 steel. A pin load cell was radially placed in direct contact with forming materials and the acquired data were compared at different workpiece locations and punch strokes with numerical simulations performed by Abaqus/Explicit code. Authors found that radial stress in the die was well predicted by numerical analyses (error consistently below 10%) and that it was not constant and fixed since it always reached a maximum value below the instantaneous position of the punch. In 2009, Plancak et al. [109] applied the FEM code Simufact Forming in the backward extrusion of an involute gear-profile made by C1121 (low carbon steel) characterized by means of the Rastegaev upsetting test. FE results showed fair agreement with experimental results (Fig. 13) despite the scattered trend of the latter related to the frequent remeshing steps.

The comparison among analytical models and FEM predictions was investigated also in 2012 by Khorasani and Valberg [110] in the extrusion of an Al alloy for two different die geometries and in different friction conditions. It

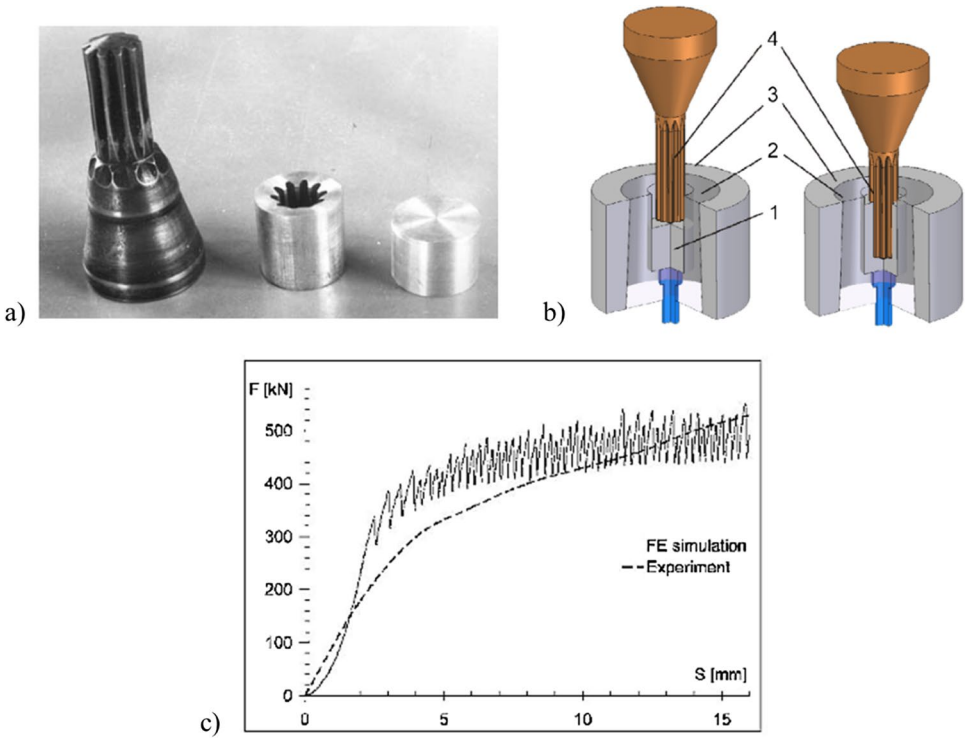

Fig. 13 a) Punch, extruded component and billet; b) simulated process; c) Comparison of experimental vs. simulated backward extrusion load [109]

was found that the formulae reported in Altan book [111] and the one proposed by Aviztur [112] are less accurate than FEA analysis with DEFORM 2D code since formulae requires simplifying assumptions deeply influencing the predicted extrusion load. In 2007, Gronostajski and Hawryluk [113] introduced the issue that numerical simulations cannot be validated only on the basis of processing load and proposed to use plastic similarity condition in order to evaluate and compare material flow during metal forming processes. In particular, they characterized different waxes composition to be compared to lead under different forming conditions and concluded that plastic similarity conditions enable an easy and quick qualitative and quantitative matching of the material flow. In 2011, Merklein et al. [114] used Simufact.Forming code to analyze the forward extrusion of a 1.0501 low carbon steel, not only as comparison to experimental data, but also for the optimization of the hardness of the final product. Indeed, geometrical features of the die (namely local deformation ratio, shoulder radius and opening angle) were varied in order to evidence the effect on the final effective strains and consequently on the product surface hardness. Austen et al. [115] presented in 2014 a paper on the reduction of the forming force of car's battery pack cell housing by means of DoE and FEM simulations The researchers used the Simufact.Forming code for 2D simplified simulations of the component under a wide range of variants involving punch's head configuration, seam geometries, distance between seams and other geometrical tool features thus showing that the shoulder length was the most significant factor. Furthermore, the paper demonstrated that forming force can be reduced by around 20% when optimal geometrical features were selected. In 2018, two papers explained that numerical simulation provides a more reliable product development in industry: Saby et al. [116] investigated the forming process of nickel-based sparkplug electrode by means of coupled thermo-mechanical simulation in order to reduce die wear whilst Gortan [117] used the same thermo-mechanical approach in order to optimize the forward extrusion of a 16MnCr5 steel under single or double stage forming sequence. A specific type of cold backward extrusion is used in the production of cans and cups. In 2008, Abrinia and Gharibi [118] applied the FEM and the upper bound approaches in order to investigate the effect of the punch shape on the process load and can wall thicknesses. A greater accuracy of the FEM method through Abaqus code was found in the comparison with experimental data and the authors also found that an optimal reduction of axial and lateral forces can be obtained with a proper selection of the punch head fillet and slope (Fig. 14). In 2017 and 2018, Henry and Liewald proposed an innovative backward cup extrusion process able to realize the cup piercing phase within a single forming stroke. In [119] the process was analyzed by means of DEFORM 2D code in order to identify the optimal punch shape and in [120] the process was validated through further numerical simulations and experimental trials on three different steel (16MnCrS5, C10C and 42CrMo4).

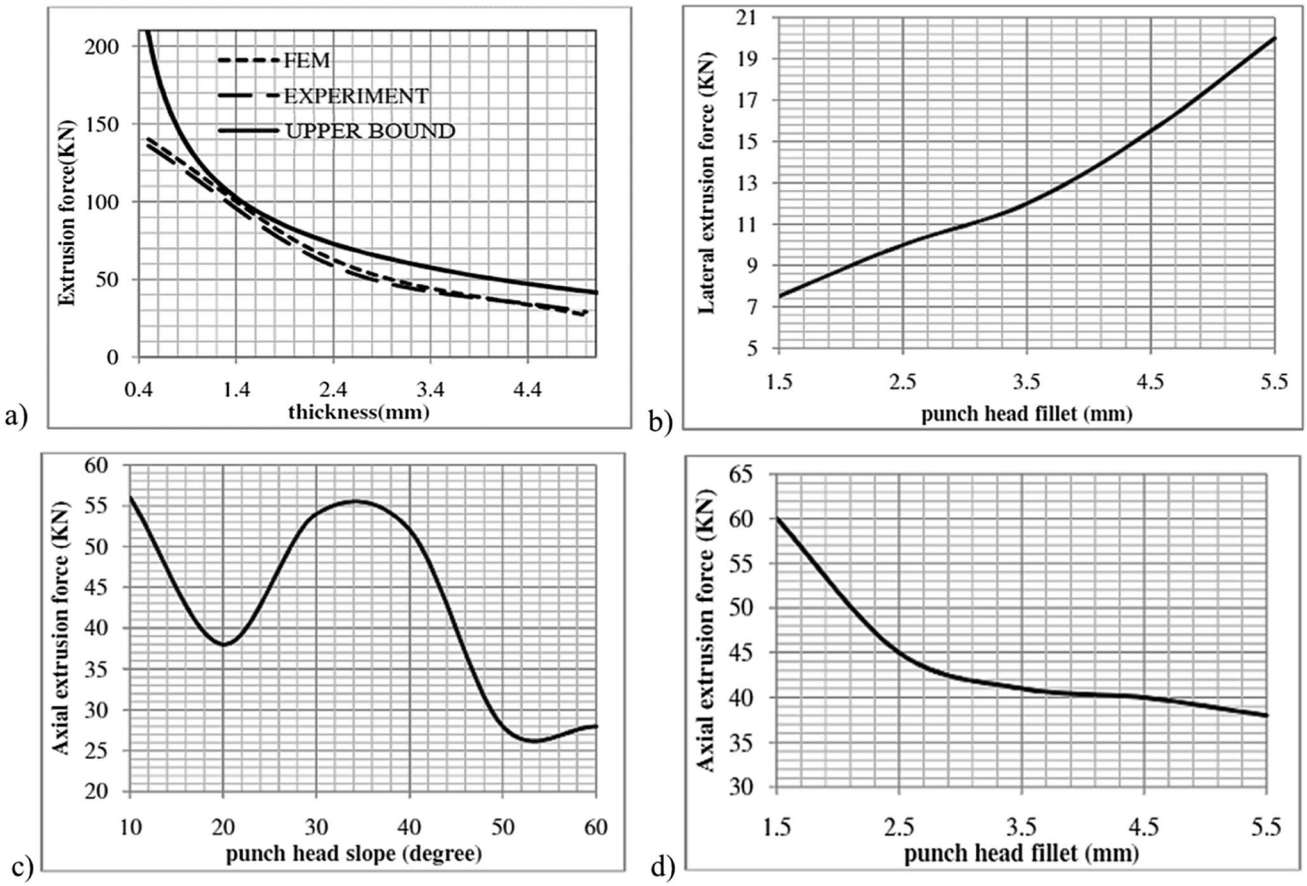

Fig. 14 a) Comparison of extrusion forces between FEM, upper bound and experimental data for various can wall thicknesses; Influence of punch head slope on b) lateral extrusion force and c) axial extrusion force; d) Influence of punch head fillet on axial extrusion load [118]

Friction and lubricants

Friction during cold forming process is a topic widely investigated by ESAFORM researchers not only for a better understanding of its effect on processing conditions but also in order to identify more reliable lubricants or to evaluate the effect of specific tailored coating on tools. In 2007, Abdollahi and Dehghani [121] developed the Matroll software able to provide several local processing parameters, including the friction coefficients (COF) during cold rolling process. The authors studied aluminum cold rolling on a four-high reversing mill and the COF provided by software was found well aligned with data previously reported in literature although the authors missed to validate the values in their experimental campaign. In 2008, Zhang et al. [122] presented the preliminary results of the activity of the WP3 workshop within the "VIF-Virtual Intelligent Forging" network aimed at providing a better understanding of the friction conditions during cold forging. In particular four University labs were involved in the study in order to compare by means of FEM simulations (FORGE software) the local friction conditions of an industrial process (cold extrusion of an AISI 1010 steel bar covered by phosphate layer and soap) with the local conditions of four different frictional tests (forward extrusion, double cup extrusion, upsetting-sliding tests and T-shape compression as reported in Fig. 15). A comparison of the tests on maximum pressure, maximum equivalent strain and new surface generation was realized and it was found that it is not possible to ensure similar contact conditions for each test and industry experiments simultaneously so a subsequent frictional test experimental campaign was planned in order to investigate which contact parameter has the greater influence on friction.

In 2014, Muller et al. [123] investigated the friction conditions during long sliding distance between workpiece and tools after multiple strokes and with different tools surface finishing by means of the sliding compression test. The authors evidenced the importance of the retained lubricant in the different conditions and the positive effect obtained with pre-lubricated tools. In 2017, two papers aimed at demonstrating the positive effect of surface functionalization for the achievement of a dry lubrication condition. Hild et al. [124] evaluated the tribological interaction between surface textured specimens and the tools in fully

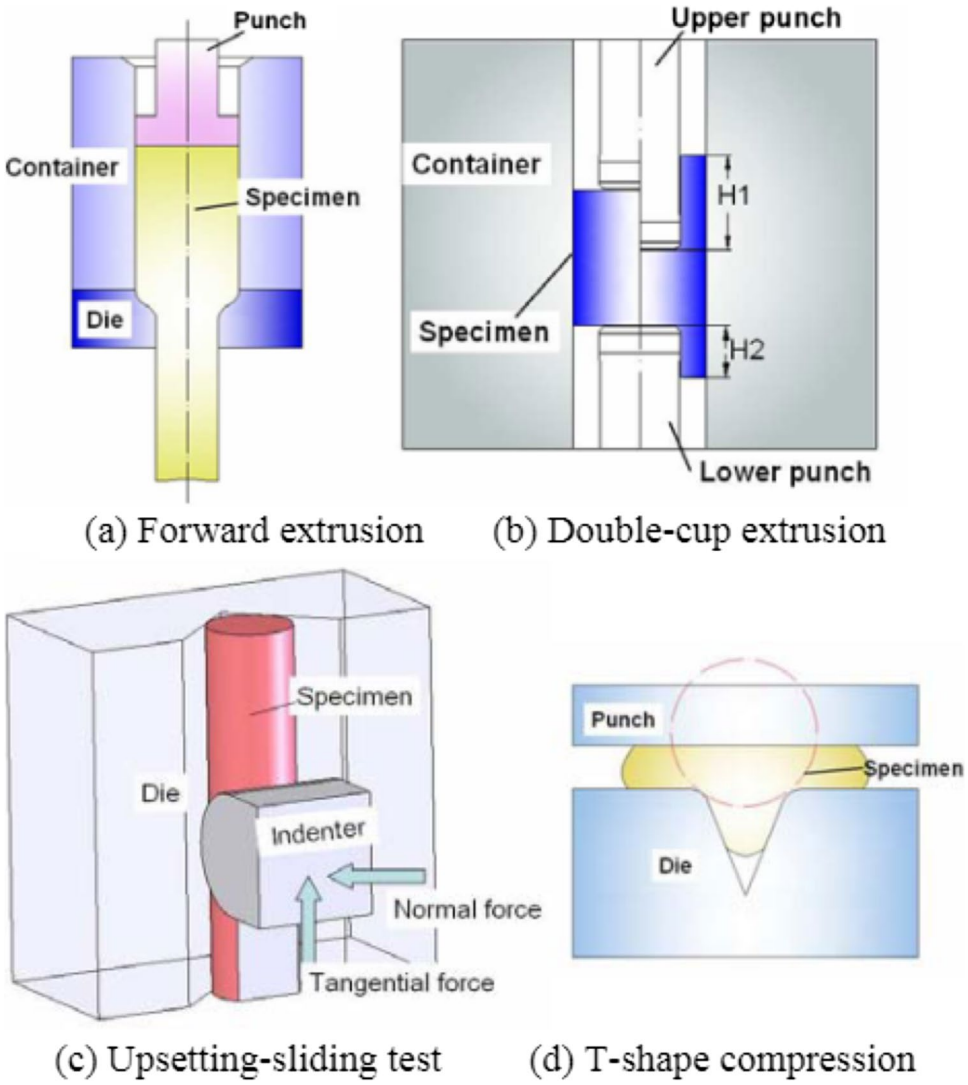

Fig. 15 Friction tests for cold forging [122]

dry conditions (forward extrusion of 42CrS4 steel workpiece over X155CrMoV12 tools) while Teller et al. [125] investigated the effect of SAM (self-assembled-monloyares obtained by octadecylphosphonic acid) tools treatment on AISI D2 and AISI H11 during pure aluminum (Al99,5%) compression-torsion wear tests. In the same year Gortan [126] observed that during several cold forming processes, including forward extrusion, temperatures may rise above 200 °C and contact pressures may exceed 2500 MPa. The author proposed an adaptive friction model able to reduce simulations errors from 18.6% (constant friction coefficient of 0.063) to 3.3% during the cold forward extrusion of C4C carbon steel. In 2020, Costa et al. [127] investigated the influence of friction models (Tresca friction factor and constant tau) in the simulation of the cold forward extrusion of an AA6082 under different lubricants (MoS2 and Soap) by means of the DEFORM 2D code. The authors evidenced that when low friction conditions are present ($m < 0.1$) both approaches provided good agreement with experimental data while at higher frictional conditions ($m > 0.1$) the constant tau approach provided better results. Finally in 2019, Idegwu et al. [128] evaluated the efficiency of different non-edible vegetable oils (Mango, water-melon, African cherry and avocado peer seeds) as lubricants during ECAP in comparison with SAE40 mineral based lubricant. Different ram speeds were tested during the deformation of an AA6063 alloy. The authors found that mango and avocado oils showed greatest potential and possibility of replacing mineral oil as industrial lubricant under all the tested ram speed being mango oil performing best, followed by SAE40, then avocado, with cherry and watermelon given the least load reducing capability.

Damage and chevron cracks

The material damage evaluation in metal forming process is of great importance in order to understand and predict the onset of some defects like the chevron cracks. Indeed, when

workpiece formability is exhausted or when the material is subject to a severe tensile stress state, cracks may originate and grow during processing stages. The following papers have experimentally and numerically investigated the prediction of the damage accumulation by means of fracture criterion. In 2009, Labergere et al. used numerical simulations (Abaqus/Explicit software) to successfully predict chevron shaped cracks in cold extrusion of 100Cr6 steel by coupling thermo-elasto-viscoplastic constitutive equations with a ductile damage model [129]. In 2013, Terhorst et al. [130] investigated a hybridized solid forward extrusion process able to prevent the onset of chevron cracks on an AISI1055 steel by means of an adequate workpiece pre-heating, a tailored online heating or a combination of both. Along the centerline of the extruded part, highest temperatures were obtained within the most tapered shaft, the location at which chevron cracks are most likely to occur. Compared to the preheating of the wrought material prior to extrusion, as usually applied in warm forming, the proposed hybridized forming process reached higher temperatures in crack-relevant areas with the same energy input. As consequence, the proposed hybridized solid forward extrusion process allowed a predefined temperature-induced increase in deformability with less energy input. In relation to the paper's achievement the same main author [131], in 2016, proposed an extension of the normalized Cockroft-Latham criterion by adding a temperature dependency to the critical damage value. Conventionally FE approaches using C-L criterion and element deletion adopt a constant value of the critical damage value. This approach may lead to an inaccurate prediction of chevron crack location and shape when high temperature ranges are involved in the forming process. The authors implemented within DEFORM 2D code a temperature dependent critical damage value through user routine and validated it through experiments on a AISI 1055 forward extrusion campaign. Figure 16 shows that, with different workpiece starting temperature, the prediction of the best chevron crack shape occurs at different critical values. A polynomial fitting was regressed by the authors and implemented in the FE simulation as material propriety thus allowing the prediction of the defect onset in a wider range of processing temperatures.

In 2019, Hearing presented two papers based on material damage modelling. In the first [132], the author investigated the effect of damage on the product performance of forward rod extruded parts. An experimental approach using automated energy dispersive X-ray spectroscopy (EDX) particle analysis in scanning electron microscopy (SEM) was used to successfully quantify the void area fraction and to obtain information on ductile damage. The method was applied on forward rod extrusion of 16MnCrS5 workpieces with varying extrusion strains and shoulder opening angles for the determination of the influence of the stress state on damage evolution. In forward rod extrusion different load paths can be realized. These load paths are characterized by scalar values describing the evolution of triaxiality during forming. The load path was described by the strain-weighted and the maximum triaxiality. The technique showed to be useful to quantify the damage state of parts, formed using various extrusion parameters. It was shown, that the triaxiality during forming is the main influencing factor for damage accumulation. Counterintuitively, higher strains do not inevitably lead to more damage. By varying the shoulder opening angles it was possible to produce parts with identical extrusion strains but different courses of triaxiality. The quantification method (SEM) proved the correlation between triaxiality and ductile damage and was verified by density measurements. It was observed, that the mean strain-weighted triaxiality describes the total volume change of a pre-existing void. A negative strain-weighted triaxiality leads to a decrease of the void area fraction. The maximum triaxiality is better suited to describe void nucleation. The results indicated that a certain threshold of the maximum triaxiality value must be exceeded for voids to nucleate. It was noted that voids below a certain threshold size are not considered. In [133] the authors illustrated the new idea to characterize material flow stress to high strains by the use of specimens obtained by forward rod extrusion. In the core of such specimens a deviatoric tension-loading was present, which is superposed by an adjustable hydrostatic pressure. Various damage levels were hence possible in the extrudate. Conducting tensile and upsetting tests with the pre-strained specimens both the influence of a load reversal as well as the material weakening through ductile damage on the resulting flow curve was explored. The results were utilized not only to identify flow curves of materials up to high strains ($\varepsilon > 1.7$), but also to get new insights into the plastic material behavior, which can be used for generating or adapting new damage models as well as kinematic hardening models under cold forging conditions. The proposed method was first assessed by means of analytical and numerical methods and then validated experimentally, by the example of the typical cold forging steel 16MnCrS5.

Residual stresses

Residual stress together with strain hardening and material damage are phenomena to be kept under control in the manufacturing of cold metal formed parts. In 2008, Statharas et al. [134] showed that residual stresses originate during cold forming processes and subsequent machining phases can be the source of premature failure of a rotary cold working die for paper cutting made by AISI D2 tool steel. In 2021, Franceschi et al. [135] investigated the role of the ejection phase of a component on the residual stresses after a forward cold extrusion process for the austenitic stainless steel AISI 316L. Experimentally, the samples were

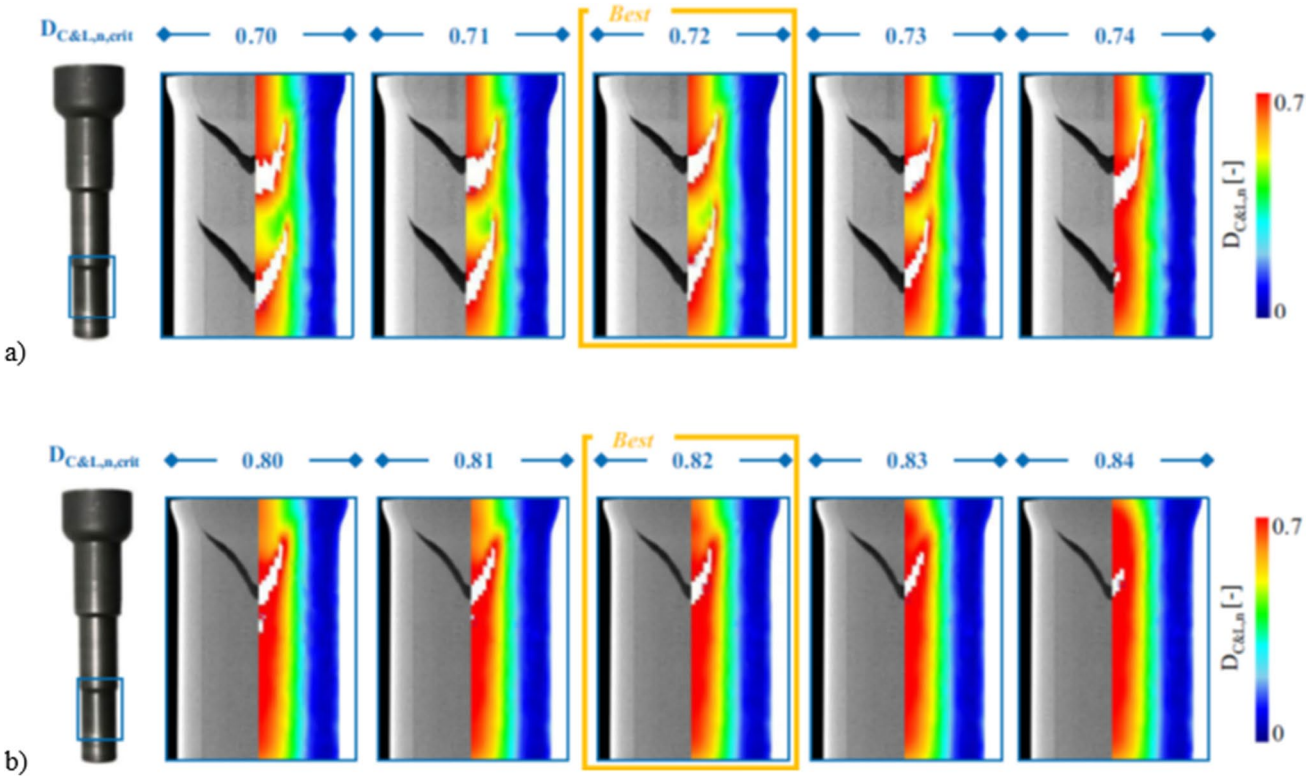

Fig. 16 Comparison of experimental and numerical chevron crack shape for different critical values a) starting forming temperature 20 °C, b) starting forming temperature 190 °C [131]

cold extruded and the residual stresses were measured in the depth through chemical material removal and X-ray diffraction. The process was also investigated through FE simulation with a combined hardening material model. A new system consisting of an active die was used in the experimental conventional cold extrusion processes and it influenced the pre-stress applied on the die during the process through the movement of four drawing cushions. This is reached through an increase of the pre-stress, which leads to compressive axial and tangential residual stresses in the near-surface region. On the other side, a decrease of the pre-stress has a detrimental effect on the axial and tangential residual stresses. The simulations could qualitatively reproduce the profile of the residual stresses found with X-ray diffraction. The ejection phase had a positive effect on the residual stresses also in the conventional technology. It was determined that the residual stresses on the surface cannot be enhanced above a definite value through the active die. Above a certain limit of pre-stress during ejection, the residual stresses tend to high tensile values. The reason for this behavior was analyzed through FE simulations. In 2007, Rossi et al. [136] evaluated the through thickness residual stresses distribution in the walls and in the corners of a cold-formed open section made of a material presenting a non-linear hardening behavior. To get results as close as possible to the reality, the complete process was modelled, including coiling and uncoiling of the sheet before the cold bending of the corner itself. The elastic spring-back after flattening as well as after final shaping were also taken into account. The material was supposed to be anisotropic and to obey to Hill's quadratic yield surface and the subsequent plastic flow rule. Nonlinear hardening behavior was taken into account in the calculations. The results confirmed a complex distribution of flexural stresses and show good agreement with measurements collected in literature.

ECAP

Sever Plastic Deformation (SPD) processes are used to increase the mechanical properties by producing grain refinement at room temperature trough high process strains. Between those processes, the Equal-Channel Angular Pressing (ECAP) is one of the most used due to the possibility of introducing large amounts of simple shear into metallic billets maintaining their initial cross sections.

In 2008, Beygelzimer et al. [137] carried out an experimental study of the Twist Extrusion (TE) of several alloys and compare it to the ECAP process in terms of deformation behavior. In 2009, Meyer et al. [138] investigated the strength, ductility and impact toughness of the AZ31B

magnesium alloy after ECAP process, with the aim to achieve an optimal and homogeneous texturing thus preventing the component to present anisotropy on the mechanical properties. In the same year, Moradi et al. [139], studied the mechanical properties of A356 aluminum alloy produced by ECAP (Fig. 17) paying attention to the effect of different heat treatments such as annealing, solution, quenching and pre/post-aging. In 2009, Olejnik et al. [140] studied the feasibility of hydrostatic extrusion (HE) of UFG AA1070, performing a sequence of ECAP and HE processes. The authors found that the sequence of operations is capable of producing high-strength, medium ductility UFG materials. In 2010, Sabirov et al. [141] verified the advantages of producing AA6061 and AA6063 components with an innovative variation of the conformal ECAP technique called ECAP with parallel channel (ECAP-PC). In 2016, Bergmann et al. [142] performed tests to investigate the Gradation Extrusion in order to increase the mechanical properties of the commercially pure Ti using this new approach as an alternative to the ECAP.

Micro-extrusion

Micro forming technologies have gained an increasing interest for the production of small metallic parts. For small production batch, machining can be the correct choice but, for the production of large quantities, forming technologies are more appropriate due to their high production rate. In this context, research activities have been carried out to investigate and solve the issues related to small scale extrusion process. In 2008, Geißdörfer et al. [143] investigated the possibility of using an ultrafine grained (UFG) metal for micro-extrusion. For this purpose, the material used was the UFG version of the pure copper, produced by severe plastic deformation (8 passes of ECAP at room temperature). The authors compared force, grain flow, shape representation and surface quality of the micro-components and assessed the benefit of using UFG structure of the metals formed. In 2009, Olejnik et al. [144] carried out experiments for the production of micro-cups of UFG Al 1070 and normal grain Al 1050 using the backward extrusion process at room temperature (Fig. 18).

In 2010, the FE simulation using Abaqus/Explicit software was used by Rosochowska et al. [145] to optimize the extrusion process configuration for the production of conical pin of Al 1070. In the following year, Berti et al. [146] performed experimental tests based on hydrostatic micro-extrusion at room temperature of billets in low carbon steel and commercially pure copper. The authors detected the effect of pressure and duration of the process on extrusion length.

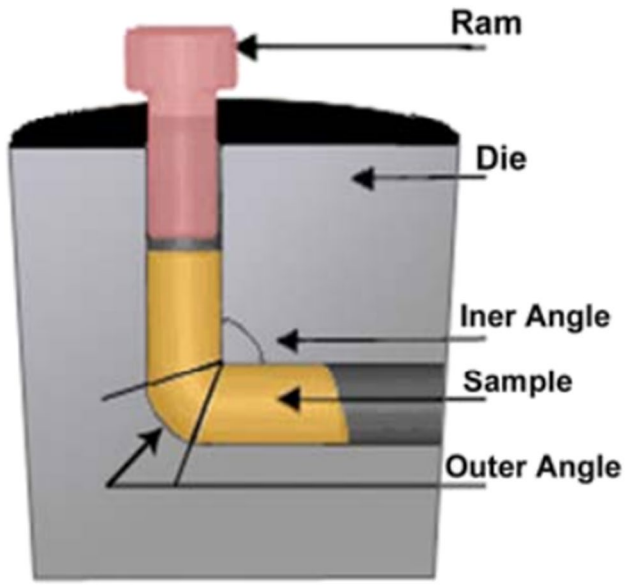

Fig. 17 Schematic of ECAP dies setup [139]

Bimetallic cold welding

In 2019, Sanabria et al. [147] carried out backward extrusions of bimetallic aluminum-copper (EN AW-1080A and Cu-ETP) and studied the friction conditions and material flow by comparing the experimental results with the FEM simulations (DEFORM code). Multiple fractures of the copper sleeve were observed in the experimental investigation, and these failures were caused by the increase of the flow stress ratio between copper and aluminum at high temperature. Moreover, the investigations showed that cold aluminum core and hot copper sleeve would reduce the flow stress ratio and lead to a more uniform material flow. In the same year, Görtan and Yaldız [148] performed a numerical investigation of the temperature, material flow, surface enlargement and contact normal stress behavior on the joint surface during co-extrusion of EN AW-6082 T6 and C10 using finite element analysis within the Abaqus/Explicit software. Three different die openings angle were simulated, and the results showed that the channel angle has no influence on the maximum temperatures on the aluminum side, but a strong influence on the steel surface maximum temperatures. Moreover, it was proved that part and die geometries have significant effect on the contact stresses and no influence on the surface enlargement on the contact interface.

Ultrasonic extrusion

In 2006, A.A.S. Akbari Mousavi and Feizi [149] investigated the effect of ultrasonic vibration on the steel forward extrusion process using the Abaqus/Explicit code, comparing the results with conventional cold forward extrusion. The authors studied the effect of extrusion speed, vibration

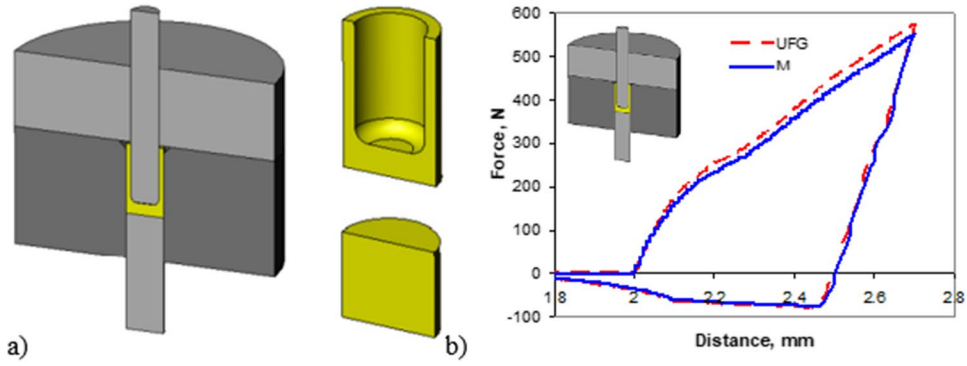

Fig. 18 a) Tool setup for backward micro-extrusion together with the billet and the extruded cup, b) Force–displacement diagram for ultra-fined grain (UFG) and Al 1050 normal grain (M) [144]

amplitude and friction conditions on the extrusion force and found that it can be reduced by decreasing the extrusion speed or by increasing the amplitude of ultrasonic vibration only if the ram velocity is lower than a critical value. In 2007, Rosochowska and Rosochowski [150] performed FE simulations using the Abaqus software of the ultrasonic backward extrusion of aluminum billets in order to investigate the influence of the vibration properties on the process parameters. Two simulations were performed, one where the die and the punch were defined as rigid bodies and the other where the punch was modelled as an elastic body. Results showed that the process velocity influences both the amplitude and the mean forming force. The latter decreases because of the reduction of the friction force due to changes in the direction and magnitude of the frictional stress over the vibration period. Moreover, the results showed a lower deflection of the elastic punch, as an indirect consequence of the reduced forming force.

Polymer extrusion

Compared to other polymer processing technologies, the main advantage of the polymer extrusion process is the possibility of continuous production of uniform cross shapes, at low cost, with high production volume and constant quality. For these reasons, polymer extrusion products have found wide application in the construction, lighting, furniture, automotive and medical fields. Due to their molecular connections, polymers have a viscoelastic mechanical behavior and, consequently, the processing of polymers presents different critical issues compared to metals. Among these issues, one of the most common is the so called "die swell" that occurs in streams of polymeric material which is forced through the die. At the exit of the die, the shape of polymer extrudate can be different from that of the die, because of the tendency of the material to recover its previous shape and volume on a microscopic scale. This complex viscoelastic behavior is the main cost driver in the design of extrusion dies.

In 2016, Siegbert et al. [151] proposed a suitable objective function for the inverse form of profile extrusion die design. They simulated the flow past the exit of the die and investigated the area downstream, developing an objective function representing die swell in the context of a non-linear non-convex continuous numerical shape optimization problem. In the context of FEM Simulation, in 2018, André et al. [152] proposed a study of the solid-state hydrostatic extrusion (SSHE) of Polymethyl-methacrylate (PMMA). By using commercial DEFORM 3D code, they compared SSHE simulation of PMMA with SSHE of the AA7108 aluminum alloy. They proved that the force–stroke curve exhibited a characteristic constitutive softening and a friction-dependent thermal softening for PMMA, and the temperature increased from a ring-shaped hot spot close to the die edge, in contrast to the typical gradual increase in temperature from the die-material interface for the aluminum alloy. Accordingly, PMMA exhibited a characteristic thermally-induced mechanical behavior, and the velocity gradient from the center to surface was higher in PMMA as compared to aluminum.

Drawing

Drawing technology is industrially applied on a wide range of materials for the production of wires, bars and tubes. Great improvements for the process optimization have been made also thanks to the development of FE (Finite Element) models able to simulate the drawing process in different configurations. However, an accurate modelling of the material deformation and friction behavior between material and tools is required to improve the effectiveness of the FE models of the process. In the past years the drawing process has been extensively studied also within ESAFORM community for the investigation of various process related aspects.

A theoretical approach to the process was proposed in 2005 by Cristescu [153] that analyzed the theory of fast material forming. He started from the Bingham theory to provide a mathematical model, first for the wire drawing,

then for the tube drawing and, at the end, for the tube extrusion. The studies carried out in the following years were supported by the numerical simulation, which, in the meantime, was becoming more consolidated. In 2007, Bruni et al. [154] developed a methodology based on a combined numerical-experimental approach to evaluate friction coefficient at the die-workpiece interface in tube drawing. The method, called Upsetting Sliding Test (UTS), consisting in sliding of an indenter on the specimen surface with a proper penetration. The experiment was conducted on tubes in desulphurized steel, lubricated using a zinc phosphate coating chemically combined with soap. In the same year, Bobadilla et al. [155], in collaboration with Trefil Europe Bourg-en-Bresse and CEMEF (Centre of Material Forming), investigated the production of high carbon steels flat wires, which includes the wire drawing followed by a rolling to change the section of the wire. In order to identify the material behavior in the case of large strains, they plotted the strain–stress curve as an assembly of several tensile tests after each pass of drawing. Finally, a damage criterion was implemented using FORGE software for the optimization of the process. Chen et al. [156], in 2008, used the rigid-plastic finite element DEFORM 2D code to investigate the drawing process and the plastic deformation behavior of a composite aluminum (A1100)-copper (CDA 110) alloy (Fig. 19). The simulations were focused on the effects of the die semi-cone angle, of the friction factor, of the diameter ratio of the composite wire, on the damage factor and on the effective strain distributions. Abaqus/Explicit software was used by Linardon et al. [157], in 2011, in their investigation of the stainless-steel platinum alloy tube cold drawing process. Also in this study, the material behavior was characterized through tensile tests at strain rates as close as possible to the high strain rates reached during the drawing process. An inverse analysis was performed to fit the friction coefficient thanks to finite element simulation and experimental drawing tests, and the Cockroft-Latham criterion was applied to understand the influence of different process parameters on tube drawing.

An approach more oriented towards the overall optimization of the different drawing stages was presented in 2011 by Thimont et al. [158]. They provided a theoretical model of the industrial wet multipass drawing process applied on high strength thin steel wires. After the definition of a constitutive law based on the wire microstructure evolution, a mechanical study of the slip-type multipass drawing machine was performed and a set of experiments was carried out to identify the friction coefficient through an inverse analysis. The model provided several wide-ranging results that can be reliably used in order to set starting conditions of the drawing machines. About critical issues and failures, one of the most common defects that can occur during cold drawing process is the central burst defect, also called chevron crack. In 2005, Koohpayeh et al. [159] studied the appearance of these defects in aluminum wire drawing. Starting from the Avitzur model,

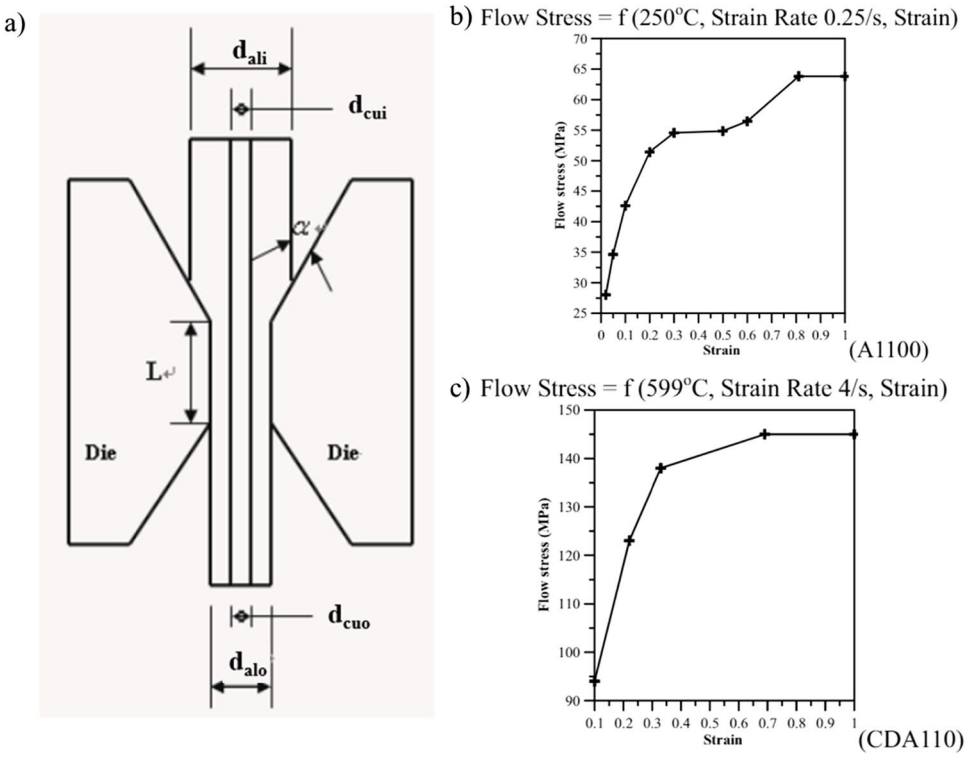

Fig. 19 a) Schematic illustration of aluminum-copper alloy wire drawing process. b) Stress–strain relationship of aluminum alloy. c) Stress–strain relationship of copper alloy [156]

they developed a new criterion for the prediction of the central burst in which, in addition to the drawing and geometrical conditions, the effect of strain-hardening exponent is involved. In the following years, Eickemeyer et al. [160] investigated the surface roughness development on magnesium and cobalt wires during the drawing process. These hcp-metals tend to be roughened in the conical part of the die and this contributes to shear cracking. An analysis on the surface roughness of the drawn products was also carried out in 2020 by Kishimoto et al. [161] in their study about micro copper tubes. They analyzed the outer diameter and surface quality of the final tubes to clarify deformation behavior of tubes in hollow sinking. Finally, Guilleaume et al. [162] presented a new concept for a hybrid deep drawing tool made by polymer concrete. The hybrid tool had a macro-structure of the blank-holder and drawing die, as implemented in the past in a steel tool for a lubricant free deep drawing process. The aim of using this innovative material was the possibility to easily integrate other functional elements like temperature and pressure sensors into the drawing die or blank-holder.

Future trends

This work presented an overview of the main advancements in extrusion and drawing in the last 25 years as captured by the dedicated section of the ESAFORM conference. From the performed analysis, many trends emerged as near future driving forces of the research such as the forming of high performances, high strength to weight ratio materials, the setting up of novel non-conventional methods and the development of multi-scale numerical models, among many others. The overall aim is to discover novel technologies able to ensure reduced consumption of materials, energy and harmful emissions but, at the same time, to provide highly efficient productions of high-quality components. This aim is pursued even through an increased robotization and automatization of the production systems, that allowed gaining repeatable narrowed tolerances as well as a fine-grained microstructures, and the development of integrated, multiscale and multiphysics twin-models of the processes. Recycling must be also forcibly listed among the driving forces since ensuring the sustainability and durability of the overall systems.

From a more global industry perspective, works must be driven towards the detection of technological solutions able to serve the emerging markets like those related to battery electric vehicles (BEV), automotive, aerospace, up to space exploration. These markets have nowadays the strength to push the research in outlining new and attractive frontiers that will lead to technological solutions at further service for all the existing markets.

Funding Open access funding provided by Alma Mater Studiorum - Università di Bologna within the CRUI-CARE Agreement.

Declarations

The Authors didn't receive any external financial support for the preparation of the present work and therefore there no conflict of interest to be declared.

Open Access This article is licensed under a Creative Commons Attribution 4.0 International License, which permits use, sharing, adaptation, distribution and reproduction in any medium or format, as long as you give appropriate credit to the original author(s) and the source, provide a link to the Creative Commons licence, and indicate if changes were made. The images or other third party material in this article are included in the article's Creative Commons licence, unless indicated otherwise in a credit line to the material. If material is not included in the article's Creative Commons licence and your intended use is not permitted by statutory regulation or exceeds the permitted use, you will need to obtain permission directly from the copyright holder. To view a copy of this licence, visit http://creativecommons.org/licenses/by/4.0/.

References

1. Mousoulis M, Tseronis D, Sideris LF, Fotopoulos FA, Medrea C (2006) Preliminary examination of the fracture surfaces of an aluminium hot extrusion die, due to the premature failure. Key Eng Mater 367:177–184. https://doi.org/10.4028/www.scientific.net/KEM.367.177
2. Irgens I, Nolte D, Valberg H (2010) Use of a shadowing tongue to reduce elastic die deflections. Int J Mater Form 3(1):399–402. https://doi.org/10.1007/s12289-010-0791-3
3. Reggiani B, Donati L, Tomesani L (2010) Evaluation of different FE simulation codes in the stress analysis of extrusion dies. Int J Mater Form 3(1):395–398. https://doi.org/10.1007/s12289-010-0790-4
4. Reggiani B, Donati L, Tomesani L (2011) Creep deformation modeling of a tool steel with a tempered martensitic structure used for extrusion dies. AIP Conf Proc 1353:437–442. https://doi.org/10.1063/1.3589554
5. Lechner S, Nitschke R, Muller S (2021) Numerical analysis of plastic die deformation during high temperature copper extrusion. ESAFORM 2021: Proceedings of the 24th International Conference on Material Forming MS03. https://doi.org/10.25518/ESAFORM21.4785
6. Donati L, Tomesani L, Shikorra M (2009) The effect of pocket shape in extrusion dies. Intl J Mater Form 2(S1):97–100. https://doi.org/10.1007/s12289-009-0454-4
7. Donati L, Ben Khalifa N, Tomesani L, Tekkaya AE (2012) Effect of porthole design and welding chamber dimensions on material flow and weld deformability of extruded aluminium profiles. Key Eng Mater 504–506:523–528. https://doi.org/10.4028/www.scientific.net/KEM.504-506.523
8. Negendank M, Taparli UA, Mueller S, Reimers W (2015) Microstructural characterization of indirectly extruded EN AW-6060 square tubes with axial variable wall thickness. Key Eng Mater 651–653:1585–1591. https://doi.org/10.4028/www.scientific.net/KEM.651-653.1585
9. Negendank M, Sanabria V, Mueller S, Reimers W (2019) Extrusion of magnesium alloy hollow profiles with axial variable wall thickness. AIP Conference Proceedings 2113, 030002 (2019); https://doi.org/10.1063/1.5112530
10. Biba N, Rezvykh R (1896) Kniazkin I (2017) Coupled modelling of aluminium profiles extrusion and product quality improvement

by means of simulation. AIP Conf Proc 1:140010. https://doi.org/10.1063/1.5008166
11. Holker R, Maase M, Ben Khalifa N, Tekkay AE (2014) Increased productivity in hot aluminum extrusion by using extrusion dies with inner cooling channels manufactured by rapid tooling. Key Eng Mat 611–612:981–988. https://doi.org/10.4028/www.scientific.net/KEM.611-612.981
12. Pelaccia R, Negozio M, Donati L, Reggiani B, Tomesani L (2020) Efficiency of conformal cooling channels inserts for extrusion dies. Procedia Manuf 47:209–216. https://doi.org/10.1016/j.promfg.2020.04.181
13. Pelaccia R, Negozio M, Reggiani B, Donati L, Tomesani L (2021) Analysis and optimization of cooling channels performances for industrial extrusion dies. ESAFORM 2021: Proceedings of the 24th International Conference on Material Forming 3686:1–11. Liège, Belgique. https://doi.org/10.25518/ESAFORM21.3686
14. P.T. Moe, W. Wajda, S. Støren, M.Lefstad and R.Flatval (2005) An Experimental and Numerical Study of Induction Heating. In: The 8th International Conference on Material Forming ESAFORM 2005 2:577–580. ISBN 973–271175–2.
15. Jäger A, Heilmann M, Misiolek WZ, Schikorra M, Tekkaya AE (2009) Influence of cooling rate on distortion and microstructure in extrusion of Al-Mg-Si alloys. Int J Mater Form 2:81. https://doi.org/10.1007/s12289-009-0451-7
16. Bikass S, Andersson B, Pilipenko A (2010) Simulation of distortion due to non-uniform cooling in aluminium extrusion process. Int J Mater Form 3:813–816. https://doi.org/10.1007/s12289-010-0894-x
17. Farjad Bastani A, Aukrust T, Brandal S (2010) Study of isothermal extrusion of aluminum using finite element simulations. Int J Mater Form 3:367–370. https://doi.org/10.1007/s12289-010-0783-3
18. Neag A, Favier V, Bigot R, Canta T, Frunza D (2007) Experimental Investigation and Numerical Simulation During Backward Extrusion of a Semi-Solid Al-Si Hypoeutectic Alloy. AIP Conf Proc 907:620–628. https://doi.org/10.1063/1.2729582
19. Knauf F, Baadjou R, Hirt G (2009) Analysis of semi-solid extrusion products made of steel alloy X210CrW12. Int J Mater Form 2(Suppl 1):733–736. https://doi.org/10.1007/s12289-009-0426-8
20. R.E. Logé, M. minville, E. Cini, A. Le Floc'h and E. Felder (2005) Development of a laboratory hot extrusion apparatus for tribology and rheology parameters identification. In: The 8th International Conference on Material Forming ESAFORM 2005 2:569–572. ISBN 973–271175–2
21. Sanabria V, Mueller S, Gall S, Reimers W (2014) Investigation of friction boundary conditions during extrusion of aluminium and magnesium alloys. Key Eng Mater 611–612:997–1004. https://doi.org/10.4028/www.scientific.net/KEM.611-612.997
22. V. Sanabria, F. Gensch and S. Mueller (2020) Application of Friction Shear Test for Constitutive Modeling Evaluation of Magnesium Alloy AZ31B at high Temperature. Procedia Manuf 47:237–244, ISSN 2351–9789. https://doi.org/10.1016/j.promfg.2020.04.205
23. Donati L, Tomesani L (2005) 3D FEM analysis of seam welds formation in aluminum extrusion and product characterization. In the Proceedings of the 8th International Conference on Material Forming, ESAFORM 2005, Cluj-Napoca, Romania, 11:561–564. ISBN 973–271173–6; 973–271175–2; 973–271174–4.
24. Donati L, Tomesani L (2007) Effect of die design on strength and deformability of hollow extruded profiles. AIP Conf Proc 907:558. https://doi.org/10.1063/1.2729572
25. Segatori A, Reggiani B, Donati L, Pinter T, Rami Y, Tomesani L (2012) Effect of process parameters on seam weld quality of ZM21 tubes. Key Eng Mater 504–506:487. https://doi.org/10.4028/www.scientific.net/KEM.504-506.487
26. Ghiotti A, Bruschi S, Dal Negro T (2005) An innovative experimental procedure to investigate seam welding in aluminium extruded profiles. In: The 8th International Conference on Material Forming ESAFORM 2005 2:553–556. ISBN 973–271175–2
27. Valberg H, Tony M, Kandis J (2011) Determining the weld quality in extrusion welding. AIP Conf Proc 1353:461–468. https://doi.org/10.1063/1.3589558
28. Dariusz L, Pawel G (2020) Estimation of extrusion welding conditions for 6xxx aluminum alloys. Procedia Manuf 47:253–260. https://doi.org/10.1016/j.promfg.2020.04.213
29. Buffa G, Donati L, Fratini L, Tomesani L (2007) Solid state bonding mechanics in extrusion and FSW: experimental tests and numerical analyses. AIP Conf Proc 907:590. https://doi.org/10.1063/1.2729577
30. Ceretti E, Mazzoni L, Guardini C (2009) Simulation of metal flow and welding prediction in porthole die extrusion: the influence of the geometrical parameters. Int J Mater Form 2:101–104. https://doi.org/10.1007/s12289-009-0494-9
31. Khan YA, Valberg H, Irgens I (2009) Joining of metal streams in extrusion welding. Int J Mater Form 2:109–112. https://doi.org/10.1007/s12289-009-0516-7
32. Khan YA, Valberg H, Irgens I (2010) Deformation conditions in the extrusion weld zone when using pointed and square ended bridge. Int J Mater Form 3(1):379–282. https://doi.org/10.1007/s12289-010-0786-0
33. Valberg H, Khan YA (2012) On the fundamental mechanism of seam welding in extrusion of aluminum alloys. Key Eng Mater 504–506. https://doi.org/10.4028/www.scientific.net/kem.504-506.529
34. Khan YA, Valberg H (2010) Metal flow in idealised a-symmetric 2D extrusion welding. Int J Mater Form 3(1):383–386. https://doi.org/10.1007/s12289-010-0787-z
35. Schwane M, Kloppenborg T, Reeb A, Ben Khalifa N (2012) Numerical approach for the evaluation of seam welding criteria in extrusion processes. Key Eng Mater 504–506:517. https://doi.org/10.4028/www.scientific.net/KEM.504-506.517
36. Schwane M, Gagliardi F, Jager A, Ben Khalifa N, Tekkaya AE (2013) Modelling approach for the determination of material flow and welding conditions in porthole die extrusion with gas pocket formation. Key Eng Mater 554–337:787–793. https://doi.org/10.4028/www.scientific.net/KEM.554-557.787
37. Gagliardi F, Ciancio C, Ambrogio G, Filice L (1896) (2017) Optimization of porthole die geometrical variables by Taguchi Method. AIP Conf Proc 1:140005. https://doi.org/10.1063/1.5008161
38. Valberg HS, Lefstad M, de Moraes Costa AL (2020) On the mechanism of formation of back-end-defects in the extrusion process. Procedia Manuf 47:245–252. https://doi.org/10.1016/j.promfg.2020.04.207
39. Negozio M, Pelaccia R, Donati L, Reggiani B, Tomesani L, Pinter T (2020) FEM Validation of front end and back end defects evolution in AA6063 and AA 6082 aluminum alloys profiles. Procedia Manuf 47:202–208. https://doi.org/10.1016/j.promfg.2020.04.178
40. Gall S, Mueller S, Reimers W (2010) Magnesium sheet production by using the extrusion process. Int J Mater Form 3(S1):371–374. https://doi.org/10.1007/s12289-010-0784-2
41. Gall S, Mueller S, Reimers W (2013) Microstructure and mechanical properties of magnesium AZ31 sheets produced by extrusion. Int J Mater Form 6:187–197. https://doi.org/10.1007/s12289-011-1069-0
42. Ge Q, Vedani M (2011) Formability of Wrought Magnesium Alloys by Hot Compression Testing and Laboratory-Scale Extrusion. AIP Conf Proc 1353:413–418. https://doi.org/10.1063/1.3589550

43. Jaehnke M, Gensch F, Mueller S (2018) Modification of the anisotropy and strength differential effect of extruded AZ31 by extrusion-shear. AIP Conf Proc 1960:030008-1–103008. https://doi.org/10.1063/1.5034851
44. Tomovic-Petrovic S, Østhus R, Jensrud O (2019) Extrusion of the magnesium-nickel alloys. AIP Conf Proc 2113:030005-1-030005–6. https://doi.org/10.1063/1.5112533
45. Flitta I, Sheppard T, Peng Z (2006) Effects of evolution of structure during and subsequent to extrusion. In: The 9th International Conference on Material Forming ESAFORM 2006 1:479–482. ISBN 83–89541–66–1
46. Krumphals F, Flitta I, Mitsche S, Wlanis T, Jahn A, Sommitsch C (2008) Comparison of experimental and Finite Element Modelling of the extrusion of AA6082 on both tools and extrudate as a function of process parameters. Int J Mater Form 1:427–430. https://doi.org/10.1007/s12289-008-0086-0
47. Parvizian F, Kayser T, Klusemann B, Svendsen B (2010) Modelling and simulation of dynamic microstructure evolution of aluminium alloys during thermomechanically coupled extrusion process. Int J Mater Form 3:363–366. https://doi.org/10.1007/s12289-010-0782-4
48. Segatori A, Foydl A, Donati L, Ben Khalifa N, Brosius A, Tomesani L, Tekkaya AE (2011) Investigation And Prediction of Grain Texture Evolution in AA6082. AIP Conf Proc 1353:449–454. https://doi.org/10.1063/1.3589556
49. Sanabria V, Mueller S (2017) Influence of Temperature and Sliding Speed on the Subsurface Microstructure Evolution of EN AW-6060 under Sticking Friction Conditions. AIP Conf Proc 1896:140012-1–10012. https://doi.org/10.1063/1.5008168
50. Koopman AJ, Geijselaers HJM, Eii NK et al (2008) Numerical flow front tracking for aluminium extrusion of a tube and a comparison with experiments. Int J Mater Form 1:423–426. https://doi.org/10.1007/s12289-008-0085-1
51. Alfaro I, Gagliardi F, Jii O et al (2009) Simulation of the extrusion of hollow profiles by natural element methods. Int J Mater Form 2:597–600. https://doi.org/10.1007/s12289-009-0614-6
52. Abrinia K, Makaremi M (2007) An upper bound solution for the spread extrusion of elliptical sections. AIP Conf Proc 907:614–619. https://doi.org/10.1063/1.2729581
53. Assaad W, Geijselaers HJM, Huétink J (2009) Boundary conditions applied on bearing corner in direct aluminum extrusion. Int J Mater Form 2:77. https://doi.org/10.1007/s12289-009-0449-1
54. Ertürk S, Steglich D, Bohlen J, Letzig D, Brocks W (2008) Modelling and Simulation of Extrusion of Magnesium Alloys. Int J Mater Form 1:419–422. https://doi.org/10.1007/s12289-008-0084-2
55. Ertürk S, Steglich D, Bohlen J, Letzig D, Brocks W (2009) THERMO-MECHANICAL MODELLING OF INDIRECT EXTRUSION PROCESS FOR MAGNESIUM ALLOYS. Int J Mater Form 2:49–52. https://doi.org/10.1007/s12289-009-0436-6
56. Donati L, Khalifa NB, Tomesani L, Tekkaya AE (2010) Comparison of different FEM code approaches in the simulation of the die deflection during aluminium extrusion. Int J Mater Form 3:375–378. https://doi.org/10.1007/s12289-010-0785-1
57. Biba N, Lishny A, Stebunov S (2011) Finite Element Modelling of Complex Thin Profile Extrusion. AIP Conf Proc 1353:425–430. https://doi.org/10.1063/1.3589552
58. Biba N, Stebunov S, Lishny A (2012) The Model for Coupled Simulation of Thin Profile Extrusion. Key Eng Mater 504–506:505–510. https://doi.org/10.4028/www.scientific.net/KEM.504-506.505
59. Kronsteiner J, Horwatitsch D (1896) Zeman K (2017) Comparison of updated Lagrangian FEM with arbitrary Lagrangian Eulerian method for 3D thermo-mechanical extrusion of a tube profile. AIP Conf Proc 140006:1–6. https://doi.org/10.1063/1.5008162
60. Caseiro JF, Valente RAF, Aii A-C et al (2010) On an Innovative Optimization Approach for the Design of Cross-section Profiles of Integrally Stiffened Panels Subjected to Elasto-plastic Buckling Deformation Modes. Int J Mater Form 3:49–52. https://doi.org/10.1007/s12289-010-0704-5
61. Siegbert R, Elgeti S, Behr M, Kurth K, Windeck C, Hopmann C (2013) Design Criteria in Numerical Design of Profile Extrusion Dies. Key Eng Mater 554–557:794–800. https://doi.org/10.4028/www.scientific.net/kem.554-557.794
62. Donati L, El Mehtedi M (2011) Characterization Of Flow Stress Of Different AA6082 Alloys By Means Of Hot Torsion Test. AIP Conf Proc 1353:455–460. https://doi.org/10.1063/1.3589557
63. Bruni C, El Mehtedi M (2012) Constitutive Equations for Finite Element Simulation. Key Eng Mater 504–506:499–504. https://doi.org/10.4028/www.scientific.net/kem.504-506.499
64. Valberg H, Misiolek W (2006) Plastic deformation in hot extrusion of an aluminum alloy characterised by FEM-analysis with experiment. In: The 9th International Conference on Material Forming ESAFORM 2006 1:587–590. ISBN 83–89541–66–1
65. Valberg H (2010) Comparison of metal flow in un-lubricated direct and indirect extrusion of aluminium alloys. Int J Mater Form 3:387–390. https://doi.org/10.1007/s12289-010-0788-y
66. Valberg H, Khorasani ST, Nolte D (2015) Comparison of the Thermo-Mechanical Conditions in an Industrial Sized Hot Aluminium Extrusion Process in Relation to those in Corresponding Small Sized Laboratory Processes. Key Eng Mater 651–653:1577–1584. https://doi.org/10.4028/www.scientific.net/KEM.651-653.1577
67. Valberg H, Costa ALM (2017) Shear zone formation within the billet and metal flow through the die orifice in unlubricated axisymmetric forward and backward extrusion. AIP Conf Proc 1896(1):140004–1–140004–7. https://doi.org/10.1063/1.5008160
68. Hansson S (2006) A three-dimensional finite element simulation of stainless steel tube extrusion using a physically based material model. In: The 9th International Conference on Material Forming ESAFORM 2006 1:475–478. ISBN 83–89541–66–1
69. Koopman AJ, Geijselaers H, Huetink J, Nilsen K, Koenis P (2007) A SUPG approach for determining frontlines in aluminium extrusion simulations and a comparison with experiments. AIP Conf Proc 907(1):602–607. https://doi.org/10.1063/1.2729579
70. Manninen T, Ramsay P, Korhonen AS (2005) Flash Formation in Conform Extrusion. In: The 8th International Conference on Material Forming ESAFORM 2005 2:557–560. ISBN 973–271175–2
71. Wajda W, Moe PT, Støren S, Lefstad M, Flatval R (2005) Measurement of Temperature and Pressure During Thin-Strip Extrusion. In: The 8th International Conference on Material Forming ESAFORM 2005 2:545–548. ISBN 973–271175–2.
72. Barton G, Kopp R (2005) Finite-Element Modeling of Hydrostatic Extrusion of Magnesium. In: The 8th International Conference on Material Forming ESAFORM 2005 2:573–576. ISBN 973–271175–2
73. Pathak K, Pagey V, Sethi V (2009) Process and die design for rod extrusion of γ iron. Int J Mater Form 2:191–196. https://doi.org/10.1007/s12289-009-0403-2
74. Valberg H (2010) Understanding material flow in aluminium extrusion by means of emptying diagrams. Int J Mater Form 3(S1):391–394. https://doi.org/10.1007/s12289-010-0789-x
75. Khan YA, Valberg H (2011) Studies of Porthole Extrusion through Die with Different Sizes of Portholes. AIP Conf Proc 1353:473–478. https://doi.org/10.1063/1.3589560

76. Kandis J, Valberg H (2012) Metal Flow in Two-Hole Extrusion of Al-Alloys Studied by FEA with Experiments. Key Eng Mater 504–506:493–498. https://doi.org/10.4028/www.scientific.net/KEM.504-506.493
77. Khorasani ST, Valberg H (2013) Velocity Field in Direct, Indirect and Friction Assisted Extrusion of Al. Key Eng Mater 554–557:776–786. https://doi.org/10.4028/www.scientific.net/KEM.554-557.776
78. Khorasani ST, Valberg H (2013) On the velocity and the strain rate field in unlubricated direct and indirect axialsymmetric extrusion of Al. Key Eng Mater 611–612:1013–1020. https://doi.org/10.4028/www.scientific.net/KEM.611.612.1013
79. Valberg H, Nolte D, Yawar K (2014) Metal Flow Conditions in Porthole Channels of Different Size. Key Eng Mater 611–612:1005–1012. https://doi.org/10.4028/www.scientific.net/KEM.611-612.1005
80. Kronsteiner J, Horwatitsch D, Hinterer A, Gusenbauer C, Zeman K (2016). Experimental determination of plastic strain in the extrusion process. 1769:140001–1–140001–6. https://doi.org/10.1063/1.4963538.
81. Chen K, Qu Y, Ding S, Liu C, Yang F (2018) Study on Numerical Simulation of Asymmetric Structure Aluminum Profile Extrusion Based on ALE Method. AIP Conf Proc 1960:030002-1-030002–6. https://doi.org/10.1063/1.5034845
82. Gaillac A, Jy C (2018) Optimized manufacture of nuclear fuel cladding tubes by FEA of hot extrusion and cold pilgering processes. AIP Conf Proc 1960:030005-1-030005–6. https://doi.org/10.1063/1.5034848
83. Valberg H, Costa ALM (2018) Metal Flow and Temperature in Direct Extrusion of Large-Size Aluminum Billets. AIP Conf Proc 1960:030011-1-030011–6. https://doi.org/10.1063/1.5034854
84. Valberg H, Lefstad M, Costa ALM (2019) The hot spot in Al-rod extrusion investigated by FEM-analysis. AIP Conf Proc 2113:030006-1-030006–6. https://doi.org/10.1063/1.5112534
85. Habans D, Olier P, Sornin D, Montmitonnet P, Mocellin K (2021) Numerical assessment of large hexagonal seamless steel tube extrusion feasibility. In: The 24th International Conference on Material Forming ESAFORM 2021. https://doi.org/10.25518/ESAFORM21.3605.
86. Chen H, Giannopoulou D, Tii G et al (2021) Homogenization of the interfacial bonding of compound-cast AA7075/6060 bilayer billets by co-extrusion. Int J Mater Form 14:1109–1119. https://doi.org/10.1007/s12289-021-01626-8
87. Negendank M, Weber C, Mueller S, Reimers W (2013) Coextrusion and Mechanical Characterization of Aluminum Coated Mg-Profiles. Key Eng Mater 554–557:767–775. https://doi.org/10.4028/www.scientific.net/kem.554-557.767
88. Sliwa R E (2006) Plastic flow of layered composite material in the extrusion process using different die geometry. In The 9th International Conference on Material Forming ESAFORM 2006, Glasgow, pp 495–498. ISBN 83–89541–66–1
89. Negendank M, Faezi H R, Ovsianytskyi O et alii (2021) Extrusion and characterization of aluminum/graphene composites. ESAFORM 2021: Proceedings of the 24th International Conference on Material Forming 3714:1–9. https://doi.org/10.25518/ESAFORM21.3714
90. Thürer SE, Uhe J (1896) Golovko O et alii (2017) Co-extrusion of semi-finished aluminium-steel compounds. AIP Conf Proc 140002:1–6. https://doi.org/10.1063/1.5008158
91. Behrens BA, Klose C, Chugreev A (1960) Thürer S E et alii (2018) Numerical investigations on the lateral angular co-extrusion of aluminium and steel. AIP Conf Proc 030001:1–6. https://doi.org/10.1063/1.5034844
92. Behrens B, Uhe J, Thürer SE, Klose C, Heimes N (2020) Development of a Modified Tool System for Lateral Angular Co-Extrusion to Improve the Quality of Hybrid Profiles. Procedia Manuf 47:224–230. https://doi.org/10.1016/j.promfg.2020.04.200
93. Foydl A, Haase M, Ben Khalifa N, Tekkaya AE (2011) Co-extrusion of Discontinuously, Non-centric Steel-reinforced Aluminum. AIP Conf Proc 1353:443–448. https://doi.org/10.1063/1.3589555
94. Foydl A, Pfeiffer I, Mii K et al (2012) Manufacturing of Steel-Reinforced Aluminum Products by Combining Hot Extrusion and Closed-Die Forging. Key Eng Mater 504–506:481–486. https://doi.org/10.4028/www.scientific.net/kem.504-506.481
95. Pietzka D, Ben Khalifa N, Gerke S, Tekkaya AE (2013) Composite Extrusion of Thin Aluminum Profiles with High Reinforcing Volume. Key Eng Mater 554–557:801–808. https://doi.org/10.4028/www.scientific.net/kem.554-557.801
96. Güley V, Ben Khalifa N, Tekkaya AE (2010) Direct recycling of 1050 aluminum alloy scrap material mixed with 6060 aluminum alloy chips by hot extrusion. Int J Mater Form 3:853–856. https://doi.org/10.1007/s12289-010-0904-z
97. Paraskevas D, Kellens K, Deng Y, Dewulf W, Kampen C (1896) Duflou J R (2017) Solid state recycling of aluminium alloys via a porthole die hot extrusion process: Scaling up to production. AIP Conf Proc 140008:1–6. https://doi.org/10.1063/1.5008164
98. Paraskevas D, Kellens K, Kampen C, Mohammadi A (1960) Duflou J R (2018) Complex deformation routes for direct recycling aluminium alloy scrap via industrial hot extrusion. AIP Conf Proc 030009:1–6. https://doi.org/10.1063/1.5034852
99. Buffa G, Campanella D, Fratini L, Micari F (2016) AZ31 magnesium alloy recycling through friction stir extrusion process. Int J Mater Form 9:613–618. https://doi.org/10.1007/s12289-015-1247-6
100. El Mehtedi M, Forcellese A, Simoncini M (1960) Spigarelli S (2018) A sustainable solid state recycling of pure aluminum by means of Friction Stir Extrusion process (FSE). AIP Conf Proc 030004:1–6. https://doi.org/10.1063/1.5034847
101. Widerøe F, Welo T (2012) An Investigation of the Material Flow in a Screw Extruder of Aluminium Using Contrast Material. Key Eng Mater 504–506:475–480. https://doi.org/10.4028/www.scientific.net/KEM.504-506.475
102. Widerøe F, Welo T, Vestal H (2013) A new testing machine to determine the behaviour of aluminium granulate under combined pressure and shear. Int J Mater Form 6:199–208. https://doi.org/10.1007/s12289-011-1070-7
103. Chatti S, Kleiner M (2007) Manufacturing of Profiles for Lightweight Structures. AIP Conf Proc 907:584–589. https://doi.org/10.1063/1.2729576
104. Moe PT, Willa-Hansen A, Støren S (2007) Optical Measurement Technology For Aluminium Extrusions. AIP Conf Proc 907:596–601. https://doi.org/10.1063/1.2729578
105. Ma X, Barnett M R (2005) An Upper Bound Analysis of Forward Extrusion through Rotating dies. In: The 8th International Conference on Material Forming ESAFORM 2005 2:565–568. ISBN 973–271175–2
106. Skakun P, Skunca M, Plancak M (2005) Radial Gear Extrusion Modelling: Analytical, Numerical and Experimental Approach. In: The 8th International Conference on Material Forming ESAFORM 2005 2:581–584. ISBN 973–271175–2
107. Pepelnjak T, Krusic V, Kuzman K (2007) Fine Coining of Bulk Metal Formed Parts in Digital Environment. AIP Conf Proc 907:578–583. https://doi.org/10.1063/1.2729575
108. Plancak M, Kuzman K, Vilotic D, Kupcrovic D (2006) Loading of dies in cold extrusion – FE simulations and experimental verification. In: The 9th International Conference on Material Forming ESAFORM 2006 1:491–494. ISBN 83–89541–66–1
109. Plančak M, Kuzman K, Vilotić D, Movrin D (2009) FE analysis and experimental investigation of cold extrusion by shaped

punch. Int J Mater Form 2(Suppl 1):117–120. https://doi.org/10.1007/s12289-009-0571-0
110. Khorasani ST, Valberg H (2012) Comparison between FEM Simulations and Analytical Calculations of Required Force for Al Extrusion. Key Eng Mater 504–506:511–516. https://doi.org/10.4028/www.scientific.net/kem.504-506.511
111. Taylan Altan (1983) Metal Forming: Fundamentals and Applications. Asm Intl., ISBN-10: 0871701677
112. Avitzur B (1968) Metal Forming: Processes and Analysis. McGraw-Hill Book Co., McGrawHill, New York, NY, USA
113. Gronostajski Z, Hawryluk M (2007) Analysis of metal forming processes by using physical modeling and new plastic similarity condition. AIP Conf Proc 907:608–613. https://doi.org/10.1063/1.2729580
114. Merklein M, Ndzomssi F, Engel U (2011) Investigation of The Influence of Tool Geometry on Effective Strain Distribution in Full Forward Extrusion. AIP Conf Proc 1353:419–424. https://doi.org/10.1063/1.3589551
115. Austen M, Noneder J, Merklein M (2014) Use of FEM and DoE to Reduce the Forming Force during Cold Extrusion of Prismatic Cell Housings. In Key Eng Mater 611–612:989–996. https://doi.org/10.4028/www.scientific.net/kem.611-612.989
116. Saby Q, Courbon C, Salvatore F, Fabre D, Romeyer F (2018) Study on the extrusion of nickel-based spark plug electrodes by numerical simulation. AIP Conf Proc 1960:030010-1-030010–6. https://doi.org/10.1063/1.5034853
117. Görtan MO (2018) Investigation of multi-stage cold forward extrusion process using coupled thermo-mechanical finite element analysis. AIP Conf Proc 1960:030006-1-030006–6. https://doi.org/10.1063/1.5034849
118. Abrinia K, Gharibi K (2008) An investigation into the backward extrusion of thin walled cans. Int J Mater Form 1:411–414. https://doi.org/10.1007/s12289-008-0082-4
119. Henry R, Liewald M (2017) Numerical study of combined process of backward cup extrusion and piercing. AIP Conf Proc 1896:140007-1-140007–5. https://doi.org/10.1063/1.5008163
120. Henry R, Liewald M (2018) Experimental study on combined cold forging process of backward cup extrusion and piercing. AIP Conf Proc 1960:030007-1-030007–6. https://doi.org/10.1063/1.5034850
121. Abdollahi H, Dehghani K (2007) Study Friction Distribution during the Cold Rolling of Material by Matroll Software. AIP Conf Proc 907:547–551. https://doi.org/10.1063/1.2729570
122. Zhang Q, Arentoft M, Bruschi, S.ii, et al (2008) Measurement of friction in a cold extrusion operation: Study by numerical simulation of four friction tests. Int J Mater Form 1:1267–1270. https://doi.org/10.1007/s12289-008-0133-x
123. Müller C, Rudel L, Yalcin D, Groche P (2014) Cold Forging with Lubricated Tools. Key Eng Mater 611–612:971–980. https://doi.org/10.4028/www.scientific.net/kem.611-612.971
124. Hild R, Feuerhack A, Trauth D, Arghavani M, Kruppe NC, Brögelmann T, Bobzin K, Klocke F (2017) Forward impact extrusion of surface textured steel blanks using coated tooling. AIP Conf Proc 1896:140009-1-140009–6. https://doi.org/10.1063/1.5008165
125. Teller M., Prünte S., Ross I, Temmler A., Schneider J.M., Hirt G. (2017) Tribological investigations of the applicability of surface functionalization for dry extrusion processes. AIP Conf Proc 1896:140001–1–140001–6 (2017) https://doi.org/10.1063/1.5008157
126. Görtan M. O. (2017) Investigation of cold extrusion process using coupled thermo-mechanical FEM analysis and adaptive friction modelling. AIP Conf Proc 1896:140011–1–140011–6 (2017) https://doi.org/10.1063/1.5008167
127. De Moraes CAL, Souza da Silva U, Valberg HS (2020) On the Friction Conditions in FEM Simulations of Cold Extrusion. Procedia Manuf 47:231–236. https://doi.org/10.1016/j.promfg.2020.04.202
128. Idegwu CU, Olaleye SA, Agboola JB, Ajiboye JS (2019) Evaluation of some non-edible vegetable oils as lubricants for conventional and non-conventional metal forming processes". AIP Conf Proc 2113:030004-1-030004–6. https://doi.org/10.1063/1.5112532
129. Labergere C, Lestriez P, Saanouni K (2009) Rassineux A (2009) Numerical simulation of bursting in extrusion process using finite viscoplasticity with ductile damage and thermal effects. Int J Mater Form 2:89. https://doi.org/10.1007/s12289-009-0428-6
130. Terhorst M, Klocke F, Niebes S, Schongen F, Mattfeld P (2013) Energy-Efficient Solid Forward Extrusion through Hybridization Based on Process-Integrated Resistance Heating. Key Eng Mater 554–557:620–629. https://doi.org/10.4028/www.scientific.net/kem.554-557.620
131. Terhorst M. Feuerhack A, Trauth D et al. (2016) Extension of the normalized Cockcroft and Latham criterion with temperature-dependent critical damage values for predicting chevron cracks in solid forward extrusion Int J Mater Form 9:449_456https://doi.org/10.1007/s12289-015-1231-1
132. Hering O, Dunlap A, Tekkaya, A.E.ii, et al (2020) Characterization of damage in forward rod extruded parts. Int J Mater Form 13:1003–1014. https://doi.org/10.1007/s12289-019-01525-z
133. Hering O, Kolpak F, Tekkaya AE (2019) Flow curves up to high strains considering load reversal and damage. Int J Mater Form 12:955–972. https://doi.org/10.1007/s12289-018-01466-z
134. Statharas D, Papageorgiou D, Sideris J. et al (2008) Preliminary examination of the fracture surfaces of a cold working die. Int J Mater Form 1:431-434https://doi.org/10.1007/s12289-008-0087-z
135. Franceschi A, Jaeger F, Hoche, H.ii, et al (2021) Calibration of the residual stresses with an active die during the ejection phase of cold extrusion. Int J Mater Form 14:223–233. https://doi.org/10.1007/s12289-020-01572-x
136. Rossi B, Habraken A-M, Pascon F (2007) On The Evaluation Of The Through Thickness Residual Stresses Distribution Of Cold Formed Profiles. AIP Conf Proc 907:570–577. https://doi.org/10.1063/1.2729574
137. Beygelzimer Y, Varyukhin V, Synkov S (2008) Shears, Vortices, and Mixing During Twist Extrusion. Inter J Mater Form 1(S1):443–446. https://doi.org/10.1007/s12289-008-0090-4
138. Meyer L, Hockauf M, Zillmann B, Schneider I (2009) Strength, ductility and impact toughness of the magnesium alloy AZ31B after equal-channel angular pressing. Int J Mater Form 2(S1):61–64. https://doi.org/10.1007/s12289-009-0545-2
139. Moradi M, Nili-Ahmadabadi M, Heidarian B (2009) Improvement of mechanical properties of AL (A356) cast alloy processed by ECAP with different heat treatments. Int J Mater Form 2(S1):85–88. https://doi.org/10.1007/s12289-009-0641-3
140. Olejnik L, Kulczyk M, Pachla W, Rosochowski A (2009) Hydrostatic extrusion of UFG aluminium. Int J Mater Form 2(S1):621–624. https://doi.org/10.1007/s12289-009-0508-7
141. Sabirov I, Perez-Prado MT, Mii M et al (2010) Application of equal channel angular pressing with parallel channels for grain refinement in aluminium alloys and its effect on deformation behavior. Int J Mater Form 3(S1):411–414. https://doi.org/10.1007/s12289-010-0794-0
142. Bergmann M, Rautenstrauch A, Rii S et al (2016) Tailoring properties of commercially pure titanium by gradation extrusion. AIP Conf Proc 1769:140002-1-140002–6. https://doi.org/10.1063/1.4963539
143. Geißdörfer S, Rosochowski A, Olejnik L, Engel U, Richert M (2008) Micro-extrusion of ultrafine grained copper. Int J Mater Form 1(S1):455–458. https://doi.org/10.1007/s12289-008-0093-1

144. Olejnik L, Presz W, Rosochowski A (2009) Backward extrusion using micro-blanked aluminium sheet. Int J Mater Form 2(S1):617–620. https://doi.org/10.1007/s12289-009-0533-6
145. Rosochowska M, Rosochowski A, Olejnik L (2010) FE simulation of micro-extrusion of a conical pin. Int J Mater Form 3(S1):423–426. https://doi.org/10.1007/s12289-010-0797-x
146. Berti G, Monti M, D'Angelo L (2011) Hydrostatic Microextrusion of Steel and Copper. AIP Conf Proc 1353:499–544. https://doi.org/10.1063/1.3589564
147. Sanabria V, Gall S, Gensch F, Nitschke R, Mueller S (2019) Backward rod extrusion of bimetallic aluminum-copper alloys at room temperature. AIP Conf Proc 2113:030001-1-030001–6. https://doi.org/10.1063/1.5112529
148. Görtan MO, Yaldız A (2019) Numerical investigations on the cold welding of aluminum and steel using forward extrusion. AIP Conf Proc 2113:030003-1-030003–6. https://doi.org/10.1063/1.5112531
149. Akbari Mousavi SAA, Feizi H (2006) Simulations of extrusion process using the ultrasonic vibrations. In: The 9th International Conference on Material Forming ESAFORM 2006 1:499–502. ISBN 83–89541–66–1.
150. Rosochowska M, Rosochowski A (2007) FE simulations of ultrasonic back extrusion. AIP Conf Proc 907:564–596. https://doi.org/10.1063/1.2729573
151. Siegbert R, Behr M, Elgeti S (2016) Die Swell as an Objective in the Design of Polymer Extrusion Dies. AIP Conf Proc 1769:140003. https://doi.org/10.1063/1.4963540
152. Costa ALM, Riffel DB, Misiolek WZ, Velberg HS (2018) A FEM simulation study of the solid state hydrostatic extrusion of PMMA. AIP Conf Proc 1960:030003. https://doi.org/10.1063/1.5034846
153. Cristescu ND (2005) Fast material forming. In: The 8th International Conference on Material Forming ESAFORM 2005 2:541–544. ISBN 973–271175–2.
154. Bruni C, Forcellese A, Gabrielli F, Simoncini M, Montelatici L (2007) Evaluation of Friction Coefficient in Tube Drawing Processes. AIP Conf Proc 907:552–557. https://doi.org/10.1063/1.2729571
155. Bobadilla C, Persem N, Foissey S (2007) Modelling of drawing and rolling of high carbon flat wires. AIP Conf Proc 907:535–540. https://doi.org/10.1063/1.2729568
156. Chen DC, Guo ZY, Wang SJ (2008) Finite element analysis of double layers alloy wire drawing processes. Int J Mater Form 1:415–418. https://doi.org/10.1007/s12289-008-0083-3
157. Linardon C, Affagard JS, Chagnon G, Favier D, Gruez B (2011) Simulation of Drawing of Small Stainless Steel Platinum Medical Tubes—Influence of the Tool Parameters on the Forming Limit. AIP Conf Proc 1353:431–436. https://doi.org/10.1063/1.3589553
158. Thimont J, Felder E, Bobadilla C, Buessler P, Persem N, Vaubourg JP (2011) Study Of The Wet Multipass Drawing Process Applied On High Strength Thin Steel Wires. AIP Conf Proc 1353:467–472. https://doi.org/10.1063/1.3589559
159. Koohpayeh SM, Taheri AK (2005) Effect of Strain-Hardening Exponent on the Occurrence of Central Burst in Aluminium Wire Drawing Process. In: The 8th International Conference on Material Forming ESAFORM 2005 2:549–552. ISBN 973–271175–2
160. Eickemeyer J, Falter M, Guth A (2006) Surface roughness and shear crack formation in cold drawing of magnesium and cobalt. In: The 9th International Conference on Material Forming ESAFORM 2006 1:483–486. ISBN 83–89541–66–1
161. Kishimoto T, Sakaguchi H, Suematsu S, Tashima K, Kajino S, Gondo S, Suzuki S (2020) Outer diameter and Surface Quality of Micro Metal Tubes in Hollow Sinking. Procedia Manuf, Volume 47, 2020, Pages 217–223, ISSN 2351–9789. https://doi.org/10.1016/j.promfg.2020.04.192.
162. Guilleaume C, Mousavi A, Brosius A (2017) Hybrid deep drawing tool for lubricant free deep drawing. AIP Conf Proc 1896:140003. https://doi.org/10.1063/1.5008159

Publisher's note Springer Nature remains neutral with regard to jurisdictional claims in published maps and institutional affiliations.